J. Fluid Mech. (2002), *vol.* 461, *pp.* 239–275. © 2002 Cambridge University Press
DOI: 10.1017/S0022112002008303 Printed in the United Kingdom

Upper bounds on general dissipation functionals in turbulent shear flows: revisiting the 'efficiency' functional

By R. R. KERSWELL

Department of Mathematics, University of Bristol, Bristol BS8 1TW, UK

(Received 5 June 2001 and in revised form 27 December 2001)

We show how the variational formulation introduced by Doering & Constantin to rigorously bound the long-time-averaged total dissipation rate $\mathbb{D}$ in turbulent shear flows can be extended to treat other long-time-averaged functionals $\limsup_{T\to\infty}(1/T)\times\int_0^T f(D,D_m,D_v)\,\mathrm{d}t$ of the total dissipation D, dissipation in the mean field D_m and dissipation in the fluctuation field D_v. Attention is focused upon the suite of functionals $f=D(D_v/D_m)^n$ and $f=D_m(D_v/D_m)^n$ $(n\geqslant 0)$ which include the 'efficiency' functional $f=D(D_v/D_m)$ (Malkus & Smith 1989; Smith 1991) and the dissipation in the mean flow $f=D_m$ (Malkus 1996) as special cases. Complementary lower estimates of the rigorous bounds are produced by generalizing Busse's multiple-boundary-layer trial function technique to the appropriate Howard–Busse variational problems built upon the usual assumption of statistical stationarity and constraints of total power balance, mean momentum balance, incompressibility and boundary conditions. The velocity field that optimizes the 'efficiency' functional is found not to capture the asymptotic structure of the observed mean flow in either plane Couette flow or plane Poiseuille flow. However, there is evidence to suppose that it is 'close' to a neighbouring functional that may.

1. Introduction

In the continued absence of any predictive theory, firm theoretical results in fluid turbulence remain a rarity. Those that do exist for inhomogeneous, anisotropic turbulence are invariably the product of variational methods which seek to find rigorous upper limits for certain global flow quantities. Although this approach dates back to the fifties (Malkus 1954, 1956), it has matured only recently with the emergence of a new variational technique discovered by Doering & Constantin (1992, 1994, 1996; Constantin & Doering 1995; Nicodemus, Grossmann & Holthaus 1997*a*, *b*). This new 'background' method, which is now known to be complementary to the classical Euler–Lagrange approach pioneered by Howard (1963, 1972, 1990) and Busse (1969*a*, *b*, 1970, 1978) (see Kerswell 1997, 1998, 2001), has not only provided new rigorous bounds (e.g. Nicodemus, Grossmann & Holthaus 1998*a*, *b*; Constantin & Doering 1999; Doering & Constantin 2001; Kerswell 2001; Plasting & Kerswell 2002) but helped put old upper bound estimates (Busse 1969*a*, 1970) on a firm footing.

The emphasis in all this work has almost exclusively been upon bounding the global transport quantity of the turbulent flow which, under statistically steady conditions or long time averaging, is equivalent to bounding the energy dissipation rate. In planar Boussinesq convection, the global transport quantity is the heat flux across

https://doi.org/10.1017/S0022112002008303 Published online by Cambridge University Press

the layer (Howard 1963, 1990; Busse 1969*a*; Chan 1971, 1974; Doering & Constantin 1996; Constantin & Doering 1999; Constantin, Hallstrom & Putkaradze 1999, 2001; Vitanov 1998, 2000*b*, *c*, *d*; Vitanov & Busse 1997, 2000; Kerswell 2001; Ierley & Worthing 2001*a*). In plane Poiseuille flow, it is the mass flux between the boundaries at constant external pressure gradient (Busse 1969*b*, 1970; Constantin & Doering 1995) and in plane Couette flow, it is the momentum transport perpendicular to the boundaries (Busse 1969*b*, 1970; Doering & Constantin 1992, 1994; Gebhardt *et al.* 1995; Nicodemus *et al.* 1997*a*, *b*, 1998*a*, *b*; Plasting & Kerswell 2002). Bounds on energy dissipation rates have also been derived in many other flow situations (e.g. general boundary-driven flows: Wang 1997, Taylor–Couette flow: Nickerson 1969; Busse 1972, plane Couette flow with suction: Doering, Spiegel & Worthing 2000, a precessing spheroid: Kerswell 1996, convection through a porous medium: Busse & Joseph 1972; Gupta & Joseph 1973; Doering & Constantin 1998; Vitanov 2000*a*, and forced periodic flow: Childress, Kerswell & Gilbert 2001; Doering & Foias 2001). Only recently has attention broadened to consider other functionals (Caulfield & Kerswell 2001; Childress *et al.* 2001).

The original reason for this focus was the physical hypothesis by Malkus (1954, 1956) that fluid flows become turbulent to maximize the approximate transport functional for the external forcing. In other words, Malkus proposed a sort of 'action' principle for turbulence in which the action was the negative of the global transport quantity so that minimizing the action corresponded to maximizing the transport. This motivated the original work by Howard and then Busse directed at seeing whether the optimal fields which emerged from suitably constrained optimization problems would bear any relation to the average features of realized turbulent flows. For shear flows, the results were encouraging as the optimizing solution contained a hierachy of realistic boundary scales, but the scaling of the dissipation bound and the internal velocity profile were not consistent with observations. For example in plane Couette flow, Busse's (1970) optimal asymptotic solution produced a maximal dissipation rate independent of the fluid viscosity as $Re \to \infty$ whereas experimental data suggest a drop off with $1/(\log Re)^2$. Furthermore, Busse's optimal asymptotic solution possessed a shear equal to one quarter of the laminar shear across the interior – Busse's famous $\frac{1}{4}$-law (now known to be a true feature of the optimization problem rather than an artifact of Busse's multiple-boundary-layer technique (Kerswell 1998)) – whereas it is generally presumed that the internal shear will vanish in the limit $Re \to \infty$. Despite these issues, the formal problem of improving Busse's (1970) thirty year old bound through either reducing the numerical coefficient or more significantly in an improved scaling continues to attract attention since it represents a well-defined route by which theoretical analysis can strive to make contact with experimental turbulence data (Busse 1978; Kerswell & Soward 1996; Nicodemus, Grossmann & Holthaus 1999; Kerswell 2000; Wang 2000; Plasting & Kerswell 2002). The path forward is clearly through incorporating further dynamical information from the Navier–Stokes equations to produce more tightly constrained variational problems. In contrast, the emphasis in the search for the 'action' functional (assuming of course that it exists) is to examine the optimal field which emerges from loosely constrained variational problems. This is because any functional will presumably start to produce realistic optimal fields if their variational problem is constrained tightly enough. Furthermore, from a practical perspective, the 'action' principle will only be useful in predicting mean turbulent statistics if its variational origins are sufficiently transparent.

Malkus & Smith (1989, hereafter referred to as MS) extended the search for an action principle to other candidate functionals beyond global transport in the context

https://doi.org/10.1017/S0022112002008303 Published online by Cambridge University Press

of plane Poiseuille flow. They developed a streamlined but rather ad-hoc variational formulation in order to survey a whole suite of different functionals based upon the statistically averaged total dissipation rate $\mathbb{D}$ and the ratio, $\mathbb{I} = \mathbb{D}_v/\mathbb{D}_m$, of statistically averaged dissipation in the fluctuation field $\mathbb{D}_v$ to dissipation in the mean flow $\mathbb{D}_m$. (The motivation to consider the quantity $\mathbb{I}$ seems to have come from a study by Ierley & Malkus (1988) which found that $\mathbb{I}$ appears to be stationary for realized flows within the context of the Reynolds & Tiederman (1967) parametrization of available data.) Within their suite of functionals $f = \mathbb{D}\mathbb{I}^n$, they discovered one functional, $\mathscr{E} := \mathbb{D}\mathbb{I}$, subsequently christened the 'efficiency' functional, which appeared to reproduce in its optimal velocity field key features of the realized turbulent mean flow. Figures 9 and 10 of MS clearly show that the optimal solution has a well-defined logarithmic sublayer close to the wall and a rapidly converging velocity defect law. The most intriguing of their figures, however, is figure 12 which shows their optimal 'prediction' closely shadowing experimental data.

Encouraging as these results are, they can only be viewed as highly suggestive since the variational problems solved in MS involve heuristic assumptions which cannot be traced back to the Navier–Stokes equations. Motivated by a need to achieve numerical solutions, their approach was to formulate a simplified variational problem based entirely upon the mean flow profile $U(z)$. This made it impossible to formally incorporate the total power balance or the mean momentum balance into their problem. Apart from expressing the efficiency functional solely in terms of U and its derivatives, the mean momentum balance was only used to generate an extended set of boundary conditions on $U(z)$ and the power balance (or dissipation rate integral as MS refer to it) to determine a minimum lengthscale in $U(z)$. The latter feature is fundamental to the MS approach since this is seen to *viscously* set the size of the innermost boundary whereas the rest of the flow domain is left free to reach an optimum amplitude *inviscidly*. All that is required of the inviscid interior is that it be inviscidly stable, which is minimally that $U''(z)$ remains one-signed (Rayleigh's criterion). MS argue plausibly that results from their variational problem should conservatively bound those from the formal problem but the relationship of their optimal fields to the formal optimal fields is tantalizingly unclear.

Further efforts to test the ability of the efficiency functional in plane Couette flow (Smith 1991) and Hagen–Poiseuille flow (Worthing 1990; Ierley & Worthing 2001*b*) have been mildly corroborative but have also tended to produce more questions than answers. Since most of these questions have revolved around how the smallest scale is chosen and the imposition of the inviscid stability condition in the interior, an examination of how the efficiency functional performs under the full set of formal constraints used by Busse (1970) seems called for. This is the underlying motivation for this paper. To achieve this objective, both the Doering–Constantin background method and Busse's multiple-boundary-layer technique have had to be applied to functionals beyond the energy dissipation rate. Showing how this can be done is the main purpose of this paper. Other work by Malkus (1996) developing ideas of statistical stability in turbulent flows has also drawn attention to the dissipation rate D_m associated with the mean flow. Formal bounds on this and the dissipation D_v associated with the fluctuation field are also found as part of this investigation.

The plan of the paper is as follows. In § 2, we introduce the canonical shear problems of plane Couette flow (PCF) and plane Poiseuille flow (PPF) which will provide the context for the ensuing variational analysis. In § 3 and Appendix A we show how Busse's multiple-boundary-layer technique may be used to produce underestimates of the upper bounds on the functionals $f = \mathbb{D}\mathbb{I}^n$ and $f = \mathbb{D}_m\mathbb{I}^n$ for $n \geqslant 0$

https://doi.org/10.1017/S0022112002008303 Published online by Cambridge University Press

using the standard dynamical constraints of total power and mean momentum balance, incompressibility and the boundary conditions. In § 4 we derive complementary overestimates of these bounds using the Doering–Constantin background approach. The closeness of the two estimates that emerge and the fact that they must bracket the true bound (see Appendix D) means that the true asymptotic behaviour of the bound and its optimizing solution is captured for all functionals considered here. Beyond the bounding results themselves, the emphasis throughout is to compare the optimal solutions that emerge with observed turbulent flows. Key features used are the structure of the interior mean profile, and the predicted scalings for $\mathbb{I}$, and the total, mean and fluctuation dissipations. The standard Prandtl–von Kármán mixing length closure, which currently appears consistent with all turbulence data, predicts that $\mathbb{I} = O(\log Re)$, $\mathbb{D} = \mathbb{D}_v = O(Re^3/(\log Re)^2)$ and $\mathbb{D}_m = O(Re^3/(\log Re)^3)$ (in viscous units) for asymptotically large Re. Conclusions are drawn in a final discussion section.

The notation used for the dissipation is as follows:

$D = \langle|\nabla \boldsymbol{u}|^2\rangle$, the total dissipation at time t (per unit mass),
$D_m = \langle \bar{\boldsymbol{u}}'^2\rangle$, the dissipation rate associated with the mean flow at time t,
$D_v = \langle|\nabla(\boldsymbol{u} - \bar{\boldsymbol{u}})|^2\rangle$, the dissipation rate associated with the velocity fluctuations,
$\mathbb{D}$ = the long time average or the statistical average of D,
$\mathbb{D}_m$ = the long time average or the statistical average of D_m,
$\mathbb{D}_v$ = the long time average or statistical average of D_v,
D_{lam} = the laminar (steady) total dissipation rate (D_{lam}^{PCF} for PCF and D_{lam}^{PPF} for PPF),
$\mathscr{D}_{max}$ = the smallest current overestimate of the upper bound on $\mathbb{D}$ produced by the Doering–Constantin approach,
D_{max} = the largest current underestimate of the upper bound on $\mathbb{D}$ produced using Busse's multiple boundary layer ansatz,
$\mathbb{D}_{max}$ = the true upper bound on the total energy dissipation subject to the constraints of total power balance, mean momentum balance, incompressibility and the boundary conditions.
$(\mathbb{I}, I) = (\mathbb{D}_v/\mathbb{D}_m, D_v/D_m)$ respectively.

2. Formulation

2.1. *Plane Couette flow*

The canonical example of boundary-driven flow is plane Couette flow in which a fluid is sandwiched between two parallel infinite plates at $z = \pm\frac{1}{2}d$ which are being moved at constant velocities $\mp\frac{1}{2}V_0\hat{\boldsymbol{x}}$ respectively. Non-dimensionalizing the system by measuring distances in units of d and velocities in viscous units of ν/d (following Busse's original work in 1970), the equations read

$$\frac{\partial \boldsymbol{u}}{\partial t} + \boldsymbol{u}\cdot\nabla\boldsymbol{u} + \nabla p = \nabla^2\boldsymbol{u} \tag{2.1}$$

with

$$\nabla\cdot\boldsymbol{u} = 0, \quad \boldsymbol{u}(x, y, \pm\tfrac{1}{2}) = \mp\tfrac{1}{2}Re, \tag{2.2}$$

https://doi.org/10.1017/S0022112002008303 Published online by Cambridge University Press

where $Re := V_0 d/\nu$. In the case of a statistically stationary turbulent flow, we adopt the Reynolds mean–fluctuation decomposition of the velocity field, $\boldsymbol{u}(\boldsymbol{x},t) = U(z)\hat{\boldsymbol{x}} + \boldsymbol{v}(\boldsymbol{x},t)$, with $\bar{\boldsymbol{v}} = \boldsymbol{0}$ where the horizontal and bulk averaging procedures are defined as

$$\bar{f} := \lim_{L_x,L_y\to\infty} \frac{1}{4L_xL_y} \int_{-L_x}^{L_x}\int_{-L_y}^{L_y} f \,\mathrm{d}x\,\mathrm{d}y, \quad \langle f\rangle := \int_{-1/2}^{1/2} \bar{f}\,\mathrm{d}z. \tag{2.3}$$

The mean momentum balance is obtained via $\overline{(2.1)\cdot\hat{\boldsymbol{x}}}$ as

$$U' = \overline{uw} - \langle uw\rangle - Re. \tag{2.4}$$

The total power balance is obtained by taking $\langle \boldsymbol{u}\cdot(2.1)\rangle$ and dropping the kinetic energy derivative term by appeal to statistical stationarity. To reflect this, we write the power balance as

$$\mathbb{D}_m + \mathbb{D}_v = \mathbb{D}, \tag{2.5}$$

where new symbols are used for each dissipation to reflect that it is a statistically averaged value. Their definitions are the same as the time-dependent functionals D_m, D_v and D except that the fluctuation velocity field is an 'average' field in some vague sense. Specifically, the statistically averaged dissipation in the fluctuation field is

$$\mathbb{D}_v := \langle|\nabla\boldsymbol{v}|^2\rangle, \tag{2.6}$$

the statistically-averaged dissipation in the mean field is

$$\mathbb{D}_m := \langle U'^2\rangle = \langle(\overline{uw} - \langle uw\rangle)^2\rangle + Re^2 \tag{2.7}$$

and the statistically averaged total dissipation (per unit mass) is

$$\mathbb{D} := \langle|\nabla\boldsymbol{u}|^2\rangle = Re^2 + Re\langle uw\rangle, \tag{2.8}$$

all in units of ν^3/d^4. The first term on the right-hand side of (2.8) represents the laminar dissipation, $D_{lam}^{PCF} := Re^2$, produced by the basic state $\boldsymbol{u} = U_{lam}\hat{\boldsymbol{x}} = -Re\,z\hat{\boldsymbol{x}}$. The second term therefore indicates the enhancement in dissipation due to turbulence and is known to dominate D_{lam}^{PCF} as $Re\to\infty$. The total power balance is then

$$Re\langle uw\rangle = \langle|\nabla\boldsymbol{v}|^2\rangle + \langle(\overline{uw} - \langle uw\rangle)^2\rangle. \tag{2.9}$$

2.2. *Plane Poiseuille flow*

The plane Poiseuille set-up we consider consists of two parallel infinite plates at $z = \pm\frac{1}{2}d$ between which fluid is driven by an applied pressure gradient of $\rho\nu^2 A/d^3$ in the $\hat{\boldsymbol{x}}$-direction. Non-dimensionalizing velocities by ν/d and distances by d gives

$$\frac{\partial\boldsymbol{u}}{\partial t} + \boldsymbol{u}\cdot\nabla\boldsymbol{u} + \nabla p = A\hat{\boldsymbol{x}} + \nabla^2\boldsymbol{u} \tag{2.10}$$

with the non-slip condition that $\boldsymbol{u} = \boldsymbol{0}$ on the plates. Adopting the Reynolds mean–fluctuation decomposition as before, then $\overline{(2.10)\cdot\hat{\boldsymbol{x}}}$ gives

$$U' = \overline{uw} - \langle uw\rangle - \frac{A}{\sqrt{12}}h(z), \tag{2.11}$$

where $h(z) := \sqrt{12}z$ so that $\langle h^2\rangle = 1$. Experimentally, the mean flow profile U is always found to be symmetric about the mid-plane. From (2.11), this implies that $\langle uw\rangle = 0$ so this is assumed henceforth. The conventional Reynolds number is

https://doi.org/10.1017/S0022112002008303 Published online by Cambridge University Press

$Re = \frac{3}{2}d[\langle U\rangle v/d]/v$ which simplifies to

$$Re = \tfrac{3}{2}\langle U\rangle = \tfrac{3}{2}\langle -zU'\rangle = \tfrac{1}{8}A - \tfrac{1}{4}\sqrt{3}\langle huw\rangle \tag{2.12}$$

and allows the mean momentum balance to be rewritten as

$$U' = \overline{uw} - h\langle huw\rangle - \tfrac{4}{3}\sqrt{3}Re\, h. \tag{2.13}$$

The statistically averaged total power balance is obtained by taking $\langle \boldsymbol{u}\cdot(2.10)\rangle$ and leads to

$$\mathbb{D}_m + \mathbb{D}_v = \mathbb{D}, \tag{2.14}$$

where the statistically averaged dissipation in the fluctuation field is

$$\mathbb{D}_v := \langle |\nabla \boldsymbol{v}|^2\rangle, \tag{2.15}$$

the statistically averaged dissipation in the mean field is

$$\mathbb{D}_m := \langle U'^2\rangle = \langle (\overline{uw} - h\langle huw\rangle)^2\rangle + \tfrac{16}{3}Re^2, \tag{2.16}$$

and the statistically averaged total dissipation (all per unit mass) is

$$\mathbb{D} := \langle |\nabla \boldsymbol{u}|^2\rangle = A\langle U\rangle = \tfrac{16}{3}Re^2 + \tfrac{4}{3}\sqrt{3}Re\langle huw\rangle, \tag{2.17}$$

all in units of v^3/d^4. The first term on the right-hand side of (2.17) represents the laminar dissipation, $D_{lam}^{PPF} := 16Re^2/3$, produced by the basic state $\boldsymbol{u} = U_{lam}\hat{\boldsymbol{x}} = \frac{1}{8}A(1-4z^2)\hat{\boldsymbol{x}}$. The second term therefore indicates the enhancement in dissipation due to turbulence and is known to dominate D_{lam}^{PPF} as $Re \to \infty$. The total power balance is then

$$\tfrac{4}{3}\sqrt{3}Re\langle huw\rangle = \langle |\nabla \boldsymbol{v}|^2\rangle + \langle (\overline{uw} - h\langle huw\rangle)^2\rangle. \tag{2.18}$$

3. Underestimating upper bounds

The variational problem of maximizing a general function of the dissipations, $f(\mathbb{D}, \mathbb{D}_m, \mathbb{D}_v)$, in plane Couette flow (PCF) and plane Poiseuille flow (PPF) may conveniently be discussed together using the generalized definitions

$$\begin{aligned} U' &:= \overline{uw} - h\langle huw\rangle - h\sqrt{D_{lam}},\\ \mathbb{D}_m &:= D_{lam} + \langle (\overline{uw} - h\langle huw\rangle)^2\rangle,\\ \mathbb{D} &:= D_{lam} + \sqrt{D_{lam}}\langle huw\rangle, \end{aligned}$$

and taking ($D_{lam} = D_{lam}^{PCF} = Re^2$, $h(z) = h_0 = h_1 = 1$) for PCF and ($D_{lam} = D_{lam}^{PPF} = 16Re^2/3$, $h(z) = \sqrt{12}z$, $h_0 = \sqrt{3}$, $h_1 = \frac{1}{2}$) for PPF. The appropriate Lagrangian for maximizing $f(\mathbb{D}, \mathbb{D}_m, \mathbb{D}_v)$ over all incompressible flow fields $\boldsymbol{v}$ which satisfy the global power balance, mean momentum balance and boundary conditions is

$$\mathscr{L} := f(\mathbb{D}, \mathbb{D}_m, \mathbb{D}_v) + \Lambda(\mathbb{D}_m + \mathbb{D}_v - \mathbb{D}) - \langle P\nabla\cdot\boldsymbol{v}\rangle \tag{3.1}$$

(the mean momentum balance is incorporated implicitly by eliminating the mean field). This leads to the Euler–Lagrange equation

$$[\alpha(\overline{uw} - h\langle huw\rangle) - \gamma h]\begin{bmatrix} w\\ 0\\ u\end{bmatrix} + \nabla p - \nabla^2\boldsymbol{v} = \boldsymbol{0} \tag{3.2}$$

https://doi.org/10.1017/S0022112002008303 Published online by Cambridge University Press

with

$$\nabla \cdot \boldsymbol{v} = 0, \quad \boldsymbol{v}(x, y, \pm\tfrac{1}{2}) = \boldsymbol{0}, \tag{3.3}$$

where

$$\alpha := \frac{\Lambda + f_{\mathbb{D}_m}}{\Lambda + f_{\mathbb{D}_v}}, \quad \gamma := \tfrac{1}{2}\sqrt{D_{lam}}\,\frac{\Lambda - f_{\mathbb{D}}}{\Lambda + f_{\mathbb{D}_v}}, \tag{3.4}$$

and, for example, $f_{\mathbb{D}} = \partial f/\partial \mathbb{D}$, $p = \frac{1}{2}P/(\Lambda + f_{\mathbb{D}_v})$. The Lagrange multiplier Λ takes the value

$$\Lambda = -\frac{(\mathbb{D} - D_{lam})f_{\mathbb{D}} + 2(\mathbb{D}_m - D_{lam})f_{\mathbb{D}_m} + \mathbb{D}_v f_{\mathbb{D}_v}}{\mathbb{D}_m - D_{lam}} \tag{3.5}$$

to ensure that $\langle \boldsymbol{v} \cdot \delta\mathscr{L}/\delta\boldsymbol{v}\rangle = 0$. The fact that γ invariably becomes large as $Re \to \infty$ for functions f of interest means that an asymptotic solution can be found using a multiple-boundary-layer technique pioneered by Busse (1969, 1970). This is developed in Appendix A for general f and used below to derive asymptotic underestimates for upper bounds on the two families of functions $f = \mathbb{D}(\mathbb{D}_v/\mathbb{D}_m)^n$ and $f = \mathbb{D}_m(\mathbb{D}_v/\mathbb{D}_m)^n$.

3.1. $f = \mathbb{D}\mathbb{I}^n$

Originally Busse found his best variational underestimate for the upper bound problem with $f = \mathbb{D}$ by taking a distinquished limit $Re \to \infty$ with $N = N(Re)$. Unfortunately, under this limiting procedure, his multi-boundary-layer solution is not strictly asymptotic since the boundary layers do not formally separate. However, the limiting sequence $\lim_{N\to\infty}\lim_{Re\to\infty}$ is valid and provides identical results. Hereafter, to avoid unnecessary complication, we apply this latter procedure implicitly. Hence, for $f = \mathbb{D}(\mathbb{D}_v/\mathbb{D}_m)^n$, the equations to be solved at asymptotically large Re are (see Appendix A)

$$\alpha = \hat{\alpha}\mu^a = \frac{1 + \dfrac{D_{lam}}{\mathbb{D}}\left(n\dfrac{\mathbb{D}}{\mathbb{D}_m} - 1\right)}{\left(1 - n - n\dfrac{\mathbb{D}_m}{\mathbb{D}_v}\right) + \dfrac{D_{lam}}{\mathbb{D}}\left(2n\dfrac{\mathbb{D}}{\mathbb{D}_m} + n\dfrac{\mathbb{D}}{\mathbb{D}_v} - 1\right)}, \tag{3.6}$$

$$4^N b_1^2 = \left(\frac{\sigma}{\beta}\right)^{3/4} h_0^{1/2}\hat{\alpha}^{1/2}\left[\frac{4^{4/3}\beta}{h_1}\right], \quad r_N = \tfrac{1}{2}(1 + a), \tag{3.7}$$

$$\mathbb{D}_v = 2\mu^{2+a-r_N}h_0h_1 4^N b_1^2, \quad \mathbb{D}_m = D_{lam} + 2\mu^{2-r_N}h_0h_1 4^N b_1^2/\hat{\alpha}, \tag{3.8}$$

$$\sqrt{D_{lam}} = 2\mu^{1-r_N}h_0h_1 4^N b_1^2\left(\frac{\mu^a\hat{\alpha} + 1}{\hat{\alpha}}\right). \tag{3.9}$$

For PCF, the asymptotic interior mean shear is given by (see (A 63))

$$U' = -\frac{Re}{2}\frac{(n+1)\mathbb{D}\mathbb{D}_m - \mathbb{D}_m^2}{\mathbb{D}\mathbb{D}_m + D_{lam}(n\mathbb{D} - \mathbb{D}_m)}. \tag{3.10}$$

For PPF, the mean velocity change across the interior is

$$\Delta U_0 = \frac{Re}{2}\frac{(n+1)\mathbb{D}\mathbb{D}_m - \mathbb{D}_m^2}{\mathbb{D}\mathbb{D}_m + D_{lam}(n\mathbb{D} - \mathbb{D}_m)} \tag{3.11}$$

so that the interior mean parabolic profile is

$$U = \tfrac{2}{3}Re + \tfrac{1}{3}\Delta U_0 - 4\Delta U_0 z^2. \tag{3.12}$$

We now consider the various scenarios as n varies.

https://doi.org/10.1017/S0022112002008303 Published online by Cambridge University Press

Case $0 \leqslant n < 1$

By inspection, the variational solution has $\mathbb{D}_m = O(\mathbb{D}_v)$ so $a = 0$ and $\hat{\alpha} = (1+n)/(1-n)$ which means that

$$f_{bound} \geqslant 2\mu^{3/2} h_0 h_1 4^N b_1^2 \hat{\alpha}^{n-1}(\hat{\alpha}+1). \tag{3.13}$$

Using (3.7) to eliminate b_1 and (3.9) to eliminate μ in favour of Re, the lower-bound expression for f_{bound} becomes

$$f_{bound} \geqslant (1+n)^{1+n}(1-n)^{1-n} D_{max}, \tag{3.14}$$

where

$$D_{max} := \frac{D_{lam}^{3/2}}{(4h_0h_1)^2}\left[\left(\frac{\sigma}{\beta}\right)^{3/4} h_0^{1/2}\left(\frac{4^{4/3}\beta}{h_1}\right)\right]^{-2} \tag{3.15}$$

is the upper bound calculated originally by Busse (1970) for the total dissipation (recovered in the special case $n = 0$). Numerically ($\beta \approx 0.624$ and $\sigma \approx 0.337$), Busse's (1970) upper bound underestimate on the total dissipation is $D_{max} := 0.01Re^3$ for PCF and $D_{max} := \frac{64}{27} \times 0.01Re^3$ for PPF. For PCF, the asymptotic interior mean shear for the optimal solution is

$$U' = -\left(\frac{3n+1}{4}\right) Re, \tag{3.16}$$

whereas for PPF, the asymptotic mean parabolic profile is

$$U = Re\left[\frac{3+n}{4} - (1+3n)z^2\right]. \tag{3.17}$$

The optimal solution has

$$[\mathbb{D}, \mathbb{D}_m, \mathbb{D}_v] = \tfrac{1}{2}(1-n^2) D_{max}[2, (1-n), (1+n)], \quad \mathbb{I} = \frac{1+n}{1-n}. \tag{3.18}$$

Case $n = 1$*: the efficiency functional*

For $n = 1$ the solution has $D_{lam} \ll \mathbb{D}_m = o(\mathbb{D}_v)$, $a = 1/5$ and $\hat{\alpha}^2 = (2h_0h_1 4^N b_1^2)^{-1}$ so

$$f_{bound} \geqslant 4D_{max} \tag{3.19}$$

and

$$\mathbb{D} = \mathbb{D}_v = 2^{4/3} D_{lam}^{1/3} D_{max}^{2/3} \sim O(Re^{8/3}), \quad \mathbb{D}_m = 2^{2/3} D_{lam}^{2/3} D_{max}^{1/3} \sim O(Re^{7/3}), \tag{3.20}$$

$$\mathbb{I} = 2^{2/3} D_{lam}^{-1/3} D_{max}^{1/3} \sim O(Re^{1/3}). \tag{3.21}$$

The asymptotic interior mean profiles for the optimal solution in both PCF and PPF are just the laminar profiles, $U' = -Re$ and $U = Re(1-4z^2)$ respectively.

Case $n > 1$

In this case, $a > 0$ implying $\mathbb{D}_m \approx 2n/(n-1) D_{lam} = o(\mathbb{D}_v)$ and α is then determined by the second expression of (3.8). For consistency, $a = 1/3$ and $\hat{\alpha} = (n-1)/(n+1)(2h_0h_1 4^N b_1^2)^{-1}$, which leads to

$$f_{bound} \geqslant 2\frac{(n-1)^{(n-1)/2}(n+1)^{(n+1)/2}}{n^n} \frac{D_{max}^{(n+1)/2}}{D_{lam}^{(n-1)/2}} \sim O(Re^{(n+5)/2}) \tag{3.22}$$

https://doi.org/10.1017/S0022112002008303 Published online by Cambridge University Press

and

$$\mathbb{D} = \mathbb{D}_v = 2\frac{(n+1)^{1/2}}{(n-1)^{1/2}} D_{max}^{1/2} D_{lam}^{1/2} \sim O(Re^{5/2}), \quad \mathbb{I} = \frac{(n^2-1)^{1/2}}{n} \frac{D_{max}^{1/2}}{D_{lam}^{1/2}} \sim O(Re^{1/2}). \tag{3.23}$$

Again, the asymptotic interior mean profiles for the optimal solution in both PCF and PPF are just the laminar profiles, $U' = -Re$ and $U = Re(1-4z^2)$ respectively.

3.2. $f = \mathbb{D}_m \mathbb{I}^n$

As before, we look for optimal asymptotic solutions valid as $Re \to \infty$. Of the expressions (3.6)–(3.9), only that for α needs changing to

$$\alpha = \hat{\alpha}\mu^a = \frac{\mathbb{D}_m + (n-1)D_{lam}}{2(\mathbb{D}_m - D_{lam})(1-n) + (\mathbb{D}_v - \mathbb{D}_m + D_{lam})n(\mathbb{D}_m/\mathbb{D}_v)}. \tag{3.24}$$

For PCF, the new expression for the asymptotic interior mean shear is now

$$U' = -\frac{Re}{2} \frac{n\mathbb{D}_m}{\mathbb{D}_m + (n-1)D_{lam}}, \tag{3.25}$$

and for PPF, the asymptotic mean parabolic profile is

$$U = Re\left[\frac{4(n-1)D_{lam} + (n+4)\mathbb{D}_m - 12n\mathbb{D}_m z^2}{6((n-1)D_{lam} + \mathbb{D}_m)}\right]. \tag{3.26}$$

Case $0 \leqslant n < 2$

For $0 \leqslant n < 2$ the solution has $\mathbb{D}_m = O(\mathbb{D}_v) \gg D_{lam}$ so $a = 0$ and $\hat{\alpha} = (1+n)/(2-n)$ which leads to

$$f_{bound} \geqslant \frac{4(1+n)^{1+n}(2-n)^{2-n}}{27} D_{max}, \tag{3.27}$$

and

$$[\mathbb{D}, \mathbb{D}_m, \mathbb{D}_v] = \tfrac{4}{27}(1+n)(2-n)D_{max}[3,(2-n),(1+n)], \quad \mathbb{I} = \frac{1+n}{2-n}. \tag{3.28}$$

Special cases are $f = \mathbb{D}_m$ $(n = 0)$ and $f = \mathbb{D}_v$ $(n = 1)$ where in both cases

$$f_{bound} \geqslant \tfrac{16}{27} D_{max}. \tag{3.29}$$

The asymptotic mean interior shear for PCF is

$$U' = -\tfrac{1}{2} nRe \tag{3.30}$$

and the interior parabolic profile

$$U = Re\left[\frac{n+4}{6} - 2nz^2\right]. \tag{3.31}$$

Case $n \geqslant 2$

For $n \geqslant 2$ we can exploit the simple relationship

$$\mathbb{D}\mathbb{I}^n = \mathbb{D}_m \mathbb{I}^n + \mathbb{D}_m \mathbb{I}^{n+1} \tag{3.32}$$

to immediately deduce the asymptotic bound for $f = \mathbb{D}_m \mathbb{I}^n$. This is possible because the bound for $f = \mathbb{D}\mathbb{I}^n$ with $n \geqslant 1$ is estimated above by a variational solution with

https://doi.org/10.1017/S0022112002008303 Published online by Cambridge University Press

$\mathbb{I} \to \infty$ as $Re \to \infty$. This implies that the asymptotic maximal values of $f = \mathbb{D}\mathbb{I}^n$ and $\mathbb{D}_m\mathbb{I}^{n+1}$ coincide. Hence for $n \geqslant 2$

$$f_{bound} \geqslant 2\frac{(n-2)^{(n-2)/2}n^{n/2}}{(n-1)^{n-1}}\frac{D_{max}^{n/2}}{D_{lam}^{(n/2)-1}} \sim O(Re^{2+(n/2)}). \tag{3.33}$$

4. Overestimating upper bounds

Here we show how the 'background' technique introduced by Doering & Constantin (1992, 1994, 1995, 1996) and subsequently improved by Nicodemus *et al.* (1997*a*, *b*) can be used to produce upper bounds on long time averages of certain classes of dissipation functionals $f(D, D_m, D_v)$. For practical purposes, the real quantity of interest is an upper bound on $f(\mathbb{D}, \mathbb{D}_m, \mathbb{D}_v)$ rather than $\limsup_{T\to\infty}(1/T)\int_0^T f(D, D_m, D_v)\,\mathrm{d}t$ however, only the latter can be bounded by the background technique. Since it is $\sup_{\boldsymbol{u}} f(D, D_m, D_v)$, where

$$\sup_{\boldsymbol{u}} f(D, D_m, D_v) \geqslant \limsup_{T\to\infty} \frac{1}{T}\int_0^T f(D, D_m, D_v)\,\mathrm{d}t, \tag{4.1}$$

that is actually bounded, if we are to find anything about $f(\mathbb{D}, \mathbb{D}_m, \mathbb{D}_v)$ then we are forced to assume

$$\sup_{\boldsymbol{u}} f(D, D_m, D_v) \geqslant f(\mathbb{D}, \mathbb{D}_m, \mathbb{D}_v). \tag{4.2}$$

In this section we secure an upper bound on $\sup_{\boldsymbol{u}} f(D, D_m, D_v)$ using the same dynamical constraints as before, that is, the total power balance, the mean momentum balance, flow incompressibility and boundary conditions. As in Doering & Constantin's original work, we adopt Hopf's (1941) idea of a degenerate or non-unique representation of the velocity field, $\boldsymbol{u} = \phi(z)\hat{\boldsymbol{x}} + \boldsymbol{v}(\boldsymbol{x}, t)$, where crucially $\bar{\boldsymbol{v}} \neq \boldsymbol{0}$ is permitted. In fact we expect only a mean flow in the $\hat{\boldsymbol{x}}$- or 1-direction so we write $\boldsymbol{u} = (\phi + \bar{v}_1)\hat{\boldsymbol{x}} + \hat{\boldsymbol{v}}$ where $\bar{\hat{\boldsymbol{v}}} = \boldsymbol{0}$. The respective dissipation definitions then become

$$D = \langle|\nabla(\phi\hat{\boldsymbol{x}} + \boldsymbol{v})|^2\rangle, \quad D_m = \langle|\phi' + \bar{v}_1'|^2\rangle, \quad D_v = \langle|\nabla\hat{\boldsymbol{v}}|^2\rangle.$$

The key step in estimating the maximum of $f(D, D_m, D_v)$ *from above* is knowing how to construct a Lagrangian that incorporates the dynamical information from the Navier–Stokes equations in the appropriate fashion. This cannot be algorithmically done as will be seen later. However, for the specific family of functions $f = Dg(I)$, the construction

$$\mathscr{L} := f(D - a\langle\boldsymbol{v}\cdot(NS)\rangle, D_m, D_v) = f\left(D - a\langle\boldsymbol{u}\cdot(NS)\rangle + a\int_{-1/2}^{1/2}\phi\overline{(NS)}_1\,\mathrm{d}z, D_m, D_v\right) \tag{4.3}$$

works where (NS) indicates the *steady* Navier–Stokes equation. Again formally, the $a\langle\boldsymbol{v}\cdot(NS)\rangle$ term should include the unsteady Navier–Stokes equations and be long time averaged. However, it is easy to show that the velocity time-derivative term vanishes under this process (Doering & Constantin 1992) and then the long time average can be dropped. Since $f_D \neq 0$, the scalar a and function $\phi(z)$ act as Lagrange multipliers to impose the dynamical constraints of total power balance,

$$\left.\frac{\delta\mathscr{L}}{\delta a}\right|_{\boldsymbol{u},\phi} = \langle\boldsymbol{u}\cdot(NS)\rangle f_D = 0, \tag{4.4}$$

https://doi.org/10.1017/S0022112002008303 Published online by Cambridge University Press

and the mean momentum balance in the $\hat{\boldsymbol{x}}$-direction,

$$\left.\frac{\delta\mathscr{L}}{\delta\phi}\right|_{\boldsymbol{u},a} = a\overline{(NS)}_1 f_D = 0, \tag{4.5}$$

respectively. Eliminating $\boldsymbol{u}$ from $\mathscr{L}$ gives

$$\mathscr{L} = f(\langle\phi'^2\rangle - \langle(a-1)|\boldsymbol{\nabla v}|^2 + a\phi' v_1 v_3 - (a-2)\phi''\bar{v}_1\rangle, \langle|\phi' + \bar{v}_1'|^2\rangle, \langle|\boldsymbol{\nabla}\hat{\boldsymbol{v}}|^2\rangle). \tag{4.6}$$

At this point, for an upper bound on f to be available, we must be able to establish that $\mathscr{L}$ has a global maximum over v for some given ϕ and a. Sufficient conditions for this are, for example, that $f_D > 0$ and f becomes negative if $D \to -\infty$. Given this, the background field ϕ must then satisfy a spectral constraint that

$$(a-1)\langle|\boldsymbol{\nabla}\hat{\boldsymbol{v}}|^2\rangle + a\langle\phi'\hat{v}_1\hat{v}_3\rangle \geqslant 0 \quad \forall\,\hat{\boldsymbol{v}} \quad \text{with} \quad \boldsymbol{\nabla}\cdot\hat{\boldsymbol{v}} = 0 \quad \text{and} \quad \hat{\boldsymbol{v}}(x,y,\pm\tfrac{1}{2}) = \boldsymbol{0}. \tag{4.7}$$

We now develop the analysis for the two particular classes of functionals $f = Dg(I)$ and $f = D_m g(I)$.

4.1. $f = Dg(I)$

We start with the case of PCF. Rather than working with the Lagrangian

$$\mathscr{L} := \langle\phi'^2 - \{(a-1)|\boldsymbol{\nabla}\hat{\boldsymbol{v}}|^2 + (a-1)\bar{v}_1'^2 + a\phi'\hat{v}_1\hat{v}_3 - (a-2)\phi''\bar{v}_1\}\rangle g(I), \tag{4.8}$$

where

$$I := \frac{D_v}{D_m} = \frac{\langle|\boldsymbol{\nabla}\hat{\boldsymbol{v}}|^2\rangle}{\langle(\phi' + \bar{v}_1')^2\rangle}, \tag{4.9}$$

it proves easier to deal with

$$\mathscr{L} \leqslant \mathscr{L}_1 := \langle\phi'^2 - \{(a-c-1)|\boldsymbol{\nabla}\hat{\boldsymbol{v}}|^2 + (a-1)\bar{v}_1'^2 - (a-2)\phi''\bar{v}_1\}\rangle g(I) \tag{4.10}$$

which bounds $\mathscr{L}$ provided the background field satisfies the spectral constraint that

$$c\langle|\boldsymbol{\nabla}\hat{\boldsymbol{v}}|^2\rangle + a\langle\phi'\hat{v}_1\hat{v}_3\rangle \geqslant 0 \quad \forall\,\hat{\boldsymbol{v}} \quad \text{with} \quad \boldsymbol{\nabla}\cdot\hat{\boldsymbol{v}} = 0 \quad \text{and} \quad \hat{\boldsymbol{v}}(x,y,\pm\tfrac{1}{2}) = \boldsymbol{0}. \tag{4.11}$$

The Doering–Constantin approach is to optimize $\mathscr{L}_1$ over $\hat{\boldsymbol{v}}$ and $\bar{v}_1$ for given ϕ, a and c. The inner product of the optimal $\hat{\boldsymbol{v}}$ with its corresponding (vanishing) variational derivative, $\langle\hat{\boldsymbol{v}}\cdot\delta\mathscr{L}_1/\delta\hat{\boldsymbol{v}}\rangle = 0$, gives the relation

$$\langle\phi'^2 - (a-1)\bar{v}_1'^2 + (a-2)\phi''\bar{v}_1\rangle = (a-c-1)\left[\frac{g}{g'}D_m + D_v\right]. \tag{4.12}$$

Optimization over $\bar{v}_1$ gives

$$\frac{\delta\mathscr{L}_1}{\delta\bar{v}_1} = 0 \Rightarrow 2[(a-1)D_m + (a-c-1)D_v]\bar{v}_1'' = -[(a-2)D_m + 2(a-c-1)D_v]\phi''. \tag{4.13}$$

This integrates to

$$U' := (\phi' + \bar{v}_1') = \frac{a}{2[(a-1) + (a-c-1)I]}(\phi' - U_{lam}') + U_{lam}', \tag{4.14}$$

where $U_{lam} := -Re\,z$. Substituting this back into the definition of D_m and (4.12) leads to the consistency relations

$$D_m - D_{lam} = \frac{a^2}{4[(a-1) + (a-c-1)I]^2}\|\phi' - U_{lam}'\|_2^2, \tag{4.15}$$

https://doi.org/10.1017/S0022112002008303 Published online by Cambridge University Press

$$(a-c-1)D_m\left[\frac{g}{g'}+I\right]+(a-1)D_m-aD_{lam}=\frac{a^2}{2[(a-1)+(a-c-1)I]}\|\phi'-U'_{lam}\|_2^2 \tag{4.16}$$

for D_m and $I=D_v/D_m$. The problem is to minimize

$$f\leqslant f_{bound}:=Dg(I)=(a-c-1)\frac{g^2}{g'}D_m \tag{4.17}$$

over $c>0$, $a>1+c$ and ϕ which satisfy the spectral constraint (4.11) with D_m and I defined implicitly by (4.15) and (4.16). The associated asymptotic interior mean profile is then given by (4.14).

For PPF, the definition of $\mathscr{L}_1$ is modified slightly to

$$\mathscr{L}_1:=\langle\phi'^2-\{(a-c-1)|\nabla\hat{\mathbf{v}}|^2+(a-1)\bar{v}_1'^2-(a-2)\phi''\bar{v}_1-\mu\bar{v}_1\}+\lambda(\tfrac{2}{3}Re-\phi)\rangle g(I) \tag{4.18}$$

to reflect the fact that now $\langle\phi\rangle=\frac{2}{3}Re$ and $\langle\bar{v}_1\rangle=0$ (see Appendix C for a detailed explanation). The analysis proceeds as in PCF except that the additional equations $\delta\mathscr{L}_1/\delta\mu=\delta\mathscr{L}_1/\delta\lambda=0$ must be invoked alongside $\delta\mathscr{L}_1/\delta\bar{v}_1=0$ to derive an expression for $\bar{v}_1$. Apart from this, all the expressions from (4.14) to (4.17) are recovered if now $U_{lam}=Re(1-4z^2)$ and $D_{lam}=16/3Re^2$ are understood. If it is assumed that ϕ' vanishes in the interior as $Re\to\infty$, then away from the boundaries

$$U'=\chi U'_{lam}:=\frac{(a-2)+2(a-c-1)I}{2[(a-1)+(a-c-1)I]}U'_{lam}, \tag{4.19}$$

implying that the resulting mean interior optimal profile is

$$U(z)=\frac{2+\chi}{3}Re-4\chi\,Re\,z^2\quad\text{as}\quad Re\to\infty. \tag{4.20}$$

We now make the specific choice $g:=I^n$ and consider the various cases over n.

Case $0\leqslant n<1$

For $0\leqslant n<1$, it is easy to show from (4.15) and (4.16) that

$$I=\frac{n}{1-n}\frac{a-1}{a-c-1},\quad D_m=\frac{a^2}{4(a-1)^2}(1-n)^2\|\phi'-U'_{lam}\|_2^2 \tag{4.21}$$

as $Re\to\infty$ so

$$f_{bound}=\inf_{a,c,\phi}\frac{a^2n^n(1-n)^{1-n}}{4(a-c-1)^n(a-1)^{1-n}}\|\phi'-U'_{lam}\|_2^2. \tag{4.22}$$

From this, minimization of f_{bound} over ϕ at fixed a and c clearly corresponds to minimizing $\|\phi'-U'_{lam}\|_2^2$. In the case of PCF, the work of Nicodemus *et al.* (1998*a*, *b*) may be used to show that

$$\inf\|\phi'-U'_{lam}\|_2^2\to 16/27\times a/c\times\mathscr{D}_{max} \tag{4.23}$$

as $Re\to\infty$ (see Appendix B: an equivalent expression may also reasonably be inferred for PPF). Then subsequent optimization over a and c ($a,c\to 3,2/(n+1)$ as $Re\to\infty$) produces the best bound

$$f\leqslant f_{bound}=(1+n)^{1+n}(1-n)^{1-n}\mathscr{D}_{max}\quad\text{as}\quad Re\to\infty, \tag{4.24}$$

where the optimal solution has

$$[D,D_m,D_v]=\tfrac{1}{2}(1-n^2)\mathscr{D}_{max}[2,(1-n),(1+n)],\quad I=\frac{1+n}{1-n}. \tag{4.25}$$

https://doi.org/10.1017/S0022112002008303 Published online by Cambridge University Press

In PCF, the associated asymptotic interior mean profile is

$$U' = -\left(\frac{3n+1}{4}\right) Re \tag{4.26}$$

whereas for PPF, the interior profile has the parabolic form

$$U = Re\left(\frac{3+n}{4} - (1+3n)z^2\right). \tag{4.27}$$

For the special case $n = 0$ when $f = D$, (4.24) reduces to $\mathscr{D}_{max}$ which, for PCF, is Nicodemus *et al.*'s (1998*a*) bound on the total dissipation of $D \leqslant 0.01087Re^3$ and the associated interior mean profile is Busse's (1970) famous $\frac{1}{4}$-shear-law result (Kerswell 1998).

Case $n = 1$: the efficiency functional

In the case of the efficiency functional, the consistency relations (4.15) and (4.16) are

$$2(a-c-1)I = \frac{(a-1)(D_m - D_{lam}) + D_{lam}}{D_{lam}}, \tag{4.28}$$

$$(D_m - D_{lam})[(a-1)D_m + aD_{lam}]^2 = a^2 D_{lam}^2 \|\phi' - U'_{lam}\|_2^2 \tag{4.29}$$

so that

$$f_{bound} = \frac{D_m[(a-1)(D_m - D_{lam}) + D_{lam}]^2}{4(a-c-1)D_{lam}^2}. \tag{4.30}$$

As $D_m \geqslant D_{lam}$, the best bound ($\forall\, Re$) is obtained through minimizing D_m, which corresponds to minimizing $\|\phi' - U'_{lam}\|_2^2$. Since this is exactly what is required when the functional is the total dissipation, the optimal background fields are related by a renormalization in the Reynolds number (see Appendix B). For asymptotically large Re, $D_m \gg D_{lam}$ and

$$f_{bound} \approx \frac{a^2}{4(a-c-1)} \|\phi' - U'_{lam}\|_2^2. \tag{4.31}$$

Using the fact that

$$\inf \|\phi' - U'_{lam}\|_2^2 \to 16/27 \times a/c \times \mathscr{D}_{max} \tag{4.32}$$

(see Appendix B), then optimizing over a and c ($a, c \to 3, 1$ as $Re \to \infty$) produces the best bound

$$f \leqslant f_{bound} = 4\mathscr{D}_{max} \quad \text{as} \quad Re \to \infty, \tag{4.33}$$

where the optimal solution has

$$D = D_v = 2^{4/3} D_{lam}^{1/3} \mathscr{D}_{max}^{2/3} \sim O(Re^{8/3}), \quad D_m = 2^{2/3} D_{lam}^{2/3} \mathscr{D}_{max}^{1/3} \sim O(Re^{7/3}), \tag{4.34}$$

$$I = 2^{2/3} D_{lam}^{-1/3} \mathscr{D}_{max}^{1/3} \sim O(Re^{1/3}). \tag{4.35}$$

Since $I \gg 1$, the associated asymptotic interior mean profiles are just the laminar states $U = U_{lam}$ for both PCF and PPF.

Case $n > 1$

For $n > 1$, $D_v \gg D_m = O(D_{lam})$ so that (4.15) and (4.16) simplify to

$$D_m = \frac{2n}{n-1} D_{lam}, \quad I = \sqrt{\frac{a^2 n}{2(a-c-1)(n+1)D_m}} \|\phi' - U'_{lam}\|_2. \tag{4.36}$$

https://doi.org/10.1017/S0022112002008303 Published online by Cambridge University Press

Then

$$f \leqslant f_{bound} = \inf_{a,c,\phi} \frac{(n-1)^{(n-1)/2}}{(n+1)^{(n+1)/2} 2^n D_{lam}^{(n-1)/2}} \frac{a^{n+1}}{(a-c-1)^n} \|\phi' - U'_{lam}\|_2^{n+1}. \tag{4.37}$$

Again using (4.23),

$$\begin{aligned} f_{bound} &\leqslant \frac{2^{2(n+1)}}{3^{3(n+1)/2}} \frac{(n-1)^{(n-1)/2}}{2^n (n+1)^{(n+1)/2}} \frac{\mathscr{D}_{max}^{(n+1)/2}}{D_{lam}^{(n-1)/2}} \inf_{a,c} \frac{a^{3(n+1)/2}}{c^{(n+1)/2}(a-c-1)^n} \\ &\leqslant 2 \frac{(n-1)^{(n-1)/2}(n+1)^{(n+1)/2}}{n^n} \frac{\mathscr{D}_{max}^{(n+1)/2}}{D_{lam}^{(n-1)/2}} \sim O(Re^{(n+5)/2}) \end{aligned} \tag{4.38}$$

at $a = 3(n+1)/2$, $c = (n+1)/2$. The optimal field has

$$D = D_v = 2 \frac{(n+1)^{1/2}}{(n-1)^{1/2}} \mathscr{D}_{max}^{1/2} D_{lam}^{1/2} \sim O(Re^{5/2}), \quad D_m = \frac{2n}{n-1} D_{lam} \sim O(Re^2), \tag{4.39}$$

$$I = \frac{(n^2-1)^{1/2}}{n} \frac{\mathscr{D}_{max}^{1/2}}{D_{lam}^{1/2}} \sim O(Re^{1/2}). \tag{4.40}$$

Again, since $I \gg 1$, the associated asymptotic interior mean profiles are just the laminar states $U = U_{lam}$ for both PCF and PPF.

4.2. $f = D_m g(I) = D_m I^n$

As observed in § 3, since

$$DI^n = D_m I^n + D_m I^{n+1}, \tag{4.41}$$

an upper bound on DI^n will also individually bound $D_m I^{n+1}$ and $D_m I^n$. For $f = D_m I^n$ with $n \geqslant 2$ we cannot do better than this but for $0 \leqslant n < 2$ improved bounds are available. For PCF, we start by defining the Lagrangian

$$\begin{aligned} \mathscr{L} &:= (D_m - a\langle \boldsymbol{v} \cdot (NS) \rangle) I^n \\ &= \frac{\langle \phi'^2 - \{a|\nabla \hat{\boldsymbol{v}}|^2 + (a-1)\bar{v}_1'^2 + a\phi' \hat{v}_1 \hat{v}_3 - (a-2)\phi'' \bar{v}_1\} \rangle \langle |\nabla \hat{\boldsymbol{v}}|^2 \rangle^n}{\langle (\phi' + \bar{v}_1')^2 \rangle^n}. \end{aligned} \tag{4.42}$$

The only difference between this Lagrangian and that in (4.8) is the coefficient of a rather than $a-1$ in the first factor of the numerator. As a result the analysis in § 4.1 carries over once any factor of $a-c-1$ is replaced by $a-c$. So the problem is to minimize

$$f \leqslant f_{bound} := D_m I^n = \frac{(a-c)}{n} D_m I^2 \tag{4.43}$$

over $c > 0$, $a > c$ and ϕ which satisfy the spectral constraint (4.11) with D_m and I defined implicitly by (4.15) and (4.16). The associated asymptotic mean shear is again given by (4.14). For PPF, there is again the slight modification of the Lagrangian to accommodate the constraints $\langle \phi \rangle = \frac{2}{3} Re$ and $\langle \bar{v}_1 \rangle = 0$ but otherwise the analysis is unchanged. The mean interior parabolic profile for the present case is also given by (4.20).

https://doi.org/10.1017/S0022112002008303 Published online by Cambridge University Press

Case $0 \leqslant n < 1$

In this case, D_v and D_m are large compared to D_{lam} and the asymptotic solutions of (4.15) and (4.16) are

$$D_m = \frac{a^2}{4(a-1)^2}(1-n)^2\|\phi' - U'_{lam}\|_2^2, \quad I = \frac{a-1}{a-c}\frac{n}{1-n}. \tag{4.44}$$

Then

$$f_{bound} = \inf_{a,c,\phi} \frac{a^2 n^n (1-n)^{1-n}}{4(a-c)^n (a-1)^{1-n}} \|\phi' - U'_{lam}\|_2^2. \tag{4.45}$$

Using the fact that

$$\inf \|\phi' - U'_{lam}\|_2^2 \to 16/27 \times a/c \times \mathscr{D}_{max} \tag{4.46}$$

(see Appendix B), then optimizing over a and c ($a, c \to 2-n, a/(1+n)$ as $Re \to \infty$) produces the best bound

$$f \leqslant f_{bound} = \frac{4(1+n)^{1+n}(2-n)^{2-n}}{27}\mathscr{D}_{max} \quad \text{as} \quad Re \to \infty, \tag{4.47}$$

where the optimal solution has

$$[D, D_m, D_v] = \tfrac{4}{27}(1+n)(2-n)\mathscr{D}_{max}[3, (2-n), (1+n)], \quad I = \frac{1+n}{2-n}. \tag{4.48}$$

The associated asymptotic mean shear in PCF is

$$U' = -\tfrac{1}{2}n\,Re \tag{4.49}$$

and the interior parabolic profile in PPF

$$U = Re\left[\frac{n+4}{6} - 2nz^2\right]. \tag{4.50}$$

For the special case $n = 0$ when $f = D_m$, (4.24) represents a bound on the dissipation in the mean

$$D_m \leqslant \tfrac{16}{27} \times \mathscr{D}_{max}. \tag{4.51}$$

The optimal asymptotic interior shear is precisely zero in this case for both PCF and PPF.

Case $n = 1$

In this case

$$2(a-c)I = \frac{(a-1)(D_m - D_{lam}) + D_{lam}}{D_{lam}}, \tag{4.52}$$

$$(D_m - D_{lam})[(a-1)D_m + aD_{lam}]^2 = a^2 D_{lam}^2 \|\phi' - U'_{lam}\|_2^2 \tag{4.53}$$

so that

$$f_{bound} = \frac{D_m[(a-1)(D_m - D_{lam}) + D_{lam}]^2}{4(a-c)D_{lam}^2}. \tag{4.54}$$

Since $D_m \geqslant D_{lam}$, the best bound ($\forall\, Re$) is obtained through minimizing D_m, which corresponds to minimizing $\|\phi' - U'_{lam}\|_2^2$. Hence, as in the case of the efficiency functional, the optimal trial background field developed by Nicodemus *et al.* (1998*a*) for maximum total dissipation is also the optimal trial background field for $f = D_m I$

https://doi.org/10.1017/S0022112002008303 Published online by Cambridge University Press

but at a different Re. For asymptotically large Re, $D_m \gg D_{lam}$ and the best bound is obtained in the limit as $a \to 1$ (see below) so

$$f_{bound} \approx \frac{a^2}{4(a-c)} \|\phi' - U'_{lam}\|_2^2. \tag{4.55}$$

Using the fact that

$$\inf \|\phi' - U'_{lam}\|_2^2 \to 16/27 \times a/c \times \mathscr{D}_{max} \tag{4.56}$$

(see Appendix B), then optimizing over c ($c \to a/2$ as $Re \to \infty$) produces the bound

$$f \leqslant f_{bound} = \frac{16a}{27}\mathscr{D}_{max} \quad \text{as} \quad Re \to \infty, \tag{4.57}$$

which is minimized over $a > 1$ as $a \to 1$ at

$$f \leqslant f_{bound} = \frac{16}{27}\mathscr{D}_{max}. \tag{4.58}$$

The optimal solution has

$$[D, D_m, D_v] = \frac{8}{27}\mathscr{D}_{max}[3,1,2], \quad I = 2, \quad a - 1 = \frac{27}{4}\frac{D_{lam}}{\mathscr{D}_{max}} \sim O(Re^{-1}). \tag{4.59}$$

The associated asymptotic interior mean profiles are just the laminar states $U = U_{lam}$ for both PCF and PPF. The fact that the optimal $a \to 1$ indicates that the global minimum can only just be reached.

Case $n > 1$

For the case $n > 1$, we are again forced to take $a \to 1$ and obtain the very conservative upper bound

$$f_{bound} = 4\frac{(n-1)^{(n-1)/2}(3n+1)^{(3n+1)/2}}{3^{3(n+1)/2}n^n(n+1)^{n+1}}\frac{\mathscr{D}_{max}^{(n+1)/2}}{D_{lam}^{(n-1)/2}} \sim O(Re^{(n+5)/2}). \tag{4.60}$$

There is then a clear gap between this bound overestimate and the underestimate secured in (3.27). To close this we are forced to reformulate the Lagrangian. In the case of PCF consider

$$\begin{aligned}\mathscr{L} &:= (D_v - a\langle \boldsymbol{v}\cdot(NS)\rangle)\left(\frac{D_v}{D_m}\right)^{n-1} \\ &= \frac{\langle -(a-1)|\nabla\hat{\boldsymbol{v}}|^2 - a\bar{v}_1'^2 - a\phi'\hat{v}_1\hat{v}_3 + a\phi''\bar{v}_1\rangle\langle|\nabla\hat{\boldsymbol{v}}|^2\rangle^{n-1}}{\langle(\phi' + \bar{v}_1')^2\rangle^{n-1}}.\end{aligned} \tag{4.61}$$

Proceeding as before, we consider

$$f \leqslant \mathscr{L}_1 := \frac{\langle -(a-c-1)|\nabla\hat{\boldsymbol{v}}|^2 - a\bar{v}_1'^2 + a\phi''\bar{v}_1\}\rangle\langle|\nabla\hat{\boldsymbol{v}}|^2\rangle^{n-1}}{\langle(\phi' + \bar{v}_1')^2\rangle^{n-1}} \tag{4.62}$$

where

$$c\langle|\nabla\hat{\boldsymbol{v}}|^2\rangle + a\langle\phi'\hat{v}_1\hat{v}_3\rangle \geqslant 0 \quad \forall\,\hat{\boldsymbol{v}} \quad \text{with} \quad \nabla\cdot\hat{\boldsymbol{v}} = 0 \quad \text{and} \quad \hat{\boldsymbol{v}}(x, y, \pm\tfrac{1}{2}) = \boldsymbol{0}. \tag{4.63}$$

Now $\langle\hat{\boldsymbol{v}}\cdot\delta\mathscr{L}_1/\delta\hat{\boldsymbol{v}}\rangle = 0$ implies the dissipation in the fluctuation field

$$D_v = D_m I = \langle|\nabla\hat{\boldsymbol{v}}|^2\rangle = \frac{n-1}{n}\frac{\langle -a\bar{v}_1'^2 + a\phi''\bar{v}_1\rangle}{a-c-1}. \tag{4.64}$$

https://doi.org/10.1017/S0022112002008303 Published online by Cambridge University Press

Optimization over $\bar{v}_1$ gives

$$\frac{\delta \mathscr{L}_1}{\delta \bar{v}_1} = 0 \Rightarrow 2[a + (a - c - 1)I]\bar{v}_1'' = -[a + 2(a - c - 1)]\phi'', \tag{4.65}$$

which upon integration yields

$$U' := (\phi' + \bar{v}_1') = \frac{a}{2[a + (a - c - 1)I]}(\phi' - U'_{lam}) + U'_{lam}. \tag{4.66}$$

The consistency relations are then

$$D_m - D_{lam} = \frac{a^2}{4[a + (a - c - 1)I]^2}\|\phi' - U'_{lam}\|_2^2, \tag{4.67}$$

$$\frac{n}{n-1}(a - c - 1)D_m I + aD_m - D_{lam} = \frac{a^2}{2[a + (a - c - 1)I]}\|\phi' - U'_{lam}\|_2^2. \tag{4.68}$$

The problem is to minimize

$$f \leqslant f_{bound} := D_m I^n = D_v I^{n-1} = \frac{(a - c - 1)}{(n - 1)} D_m I^n \tag{4.69}$$

over $c > 0$, $a > 1 + c$ and ϕ which satisfy the spectral constraint (4.11) with D_m and I defined implicitly by (4.67) and (4.68). The associated asymptotic mean interior shear in PCF is given by

$$U' = \frac{a}{2[a + (a - c - 1)I]}(\phi' - U'_{lam}) + U'_{lam}. \tag{4.70}$$

Again, if it is assumed that ϕ' vanishes in the interior as $Re \to \infty$ in PPF, then away from the boundaries

$$U' = \chi U'_{lam} := \frac{a + 2(a - c - 1)I}{2[a + (a - c - 1)I]} U'_{lam}, \tag{4.71}$$

implying that the resulting mean interior optimal profile is

$$U(z) = \frac{2 + \chi}{3} Re - 4\chi\, Re\, z^2 \quad \text{as} \quad Re \to \infty. \tag{4.72}$$

Case $1 < n < 2$

When $1 < n < 2$, D_v and D_m are large compared to D_{lam} and the asymptotic solutions of (4.67) and (4.68) are

$$D_m = \frac{(2 - n)^2}{4}\|\phi' - U'_{lam}\|_2^2, \quad I = \frac{n - 1}{2 - n}\frac{a}{a - c - 1}. \tag{4.73}$$

Then

$$\begin{aligned} f_{bound} &= \inf_{a,c,\phi} \frac{a^n (n-1)^{n-1}(2-n)^{2-n}}{4(a - c - 1)^{n-1}}\|\phi' - U'_{lam}\|_2^2 \\ &\leqslant \inf_{a,c} \frac{a^{n+1}(n-1)^{n-1}(2-n)^{2-n}}{4c(a - c - 1)^{n-1}} \times \frac{16}{27} \times \mathscr{D}_{max}. \end{aligned} \tag{4.74}$$

Optimising over a and c ($a \to 1 + n$, $c \to 1$) as $Re \to \infty$ produces the best bound

$$f_{bound} \leqslant \tfrac{4}{27}(1 + n)^{1+n}(2 - n)^{2-n}\mathscr{D}_{max} \quad \text{as} \quad Re \to \infty, \tag{4.75}$$

https://doi.org/10.1017/S0022112002008303 Published online by Cambridge University Press

where the optimal solution has

$$[D, D_m, D_v] = \tfrac{4}{27}(1+n)(2-n)\mathscr{D}_{max}[3,(2-n),(1+n)], \quad I = \frac{1+n}{2-n}. \tag{4.76}$$

The associated asymptotic interior mean shear in PCF is

$$U' = -\tfrac{1}{2}n\,Re \tag{4.77}$$

and the interior parabolic profile in PPF

$$U = Re\left[\frac{n+4}{6} - 2nz^2\right]. \tag{4.78}$$

Case $n \geqslant 2$

For $n \geqslant 2$ we can exploit the simple relationship

$$DI^n = D_m I^n + D_m I^{n+1} \tag{4.79}$$

to immediately deduce the asymptotic bound for $f = D_m I^n$. This is possible because the bound for $f = DI^n$ with $n \geqslant 1$ is estimated above by a variational solution with $I \to \infty$ as $Re \to \infty$. This implies that the asymptotic maximal values of $f = DI^n$ and $D_m I^{n+1}$ coincide. Hence for $n \geqslant 2$

$$f_{bound} \leqslant 2\frac{(n-2)^{(n-2)/2}n^{n/2}}{(n-1)^{n-1}}\frac{\mathscr{D}_{max}^{n/2}}{D_{lam}^{(n/2)-1}} \sim O(Re^{2+(n/2)}), \tag{4.80}$$

where $a, c \to 3n/2, n/2$. The associated asymptotic interior mean profiles are just the laminar states $U = U_{lam}$ for both PCF and PPF.

5. Discussion

The formal result of this paper is the following theorem.

THEOREM 1. *For plane Poiseuille flow (PPF) and plane Couette flow (PCF), using the constraints of total power balance, mean momentum balance, fluid incompressibility and the boundary conditions, the following asymptotic bounds exist at large Re:*

$$\limsup_{T\to\infty}\frac{1}{T}\int_0^T D\left(\frac{D_v}{D_m}\right)^n \mathrm{d}t \leqslant \begin{cases} (1+n)^{n+1}(1-n)^{1-n}\mathbb{D}_{max} & 0 \leqslant n < 1 \\ 2\dfrac{(n-1)^{(n-1)/2}(n+1)^{(n+1)/2}}{n^n}\dfrac{\mathbb{D}_{max}^{(n+1)/2}}{D_{lam}^{(n-1)/2}} & 1 \leqslant n, \end{cases} \tag{5.1}$$

$$\limsup_{T\to\infty}\frac{1}{T}\int_0^T D_m\left(\frac{D_v}{D_m}\right)^n \mathrm{d}t \leqslant \begin{cases} \tfrac{4}{27}(1+n)^{n+1}(2-n)^{2-n}\mathbb{D}_{max} & 0 \leqslant n < 2 \\ 2\dfrac{(n-2)^{(n-2)/2}n^{n/2}}{(n-1)^{n-1}}\dfrac{\mathbb{D}_{max}^{n/2}}{D_{lam}^{(n-2)/2}} & 2 \leqslant n, \end{cases} \tag{5.2}$$

where D, D_m and D_v are the instantaneous total dissipation and dissipations in the mean and fluctuation fields, $\mathbb{D}_{max}$ is the maximal total dissipation under the same constraints and D_{lam} is the laminar total dissipation. For PCF, it is known that†

$$0.01Re^3 \approx D_{max} \leqslant \mathbb{D}_{max} \leqslant \mathscr{D}_{max} = 0.01087Re^3 \tag{5.3}$$

† Recent numerical calculations actually indicate that $\mathbb{D}_{max} \approx 0.0086Re^3$ – see Plasting & Kerswell (2002).

https://doi.org/10.1017/S0022112002008303 Published online by Cambridge University Press

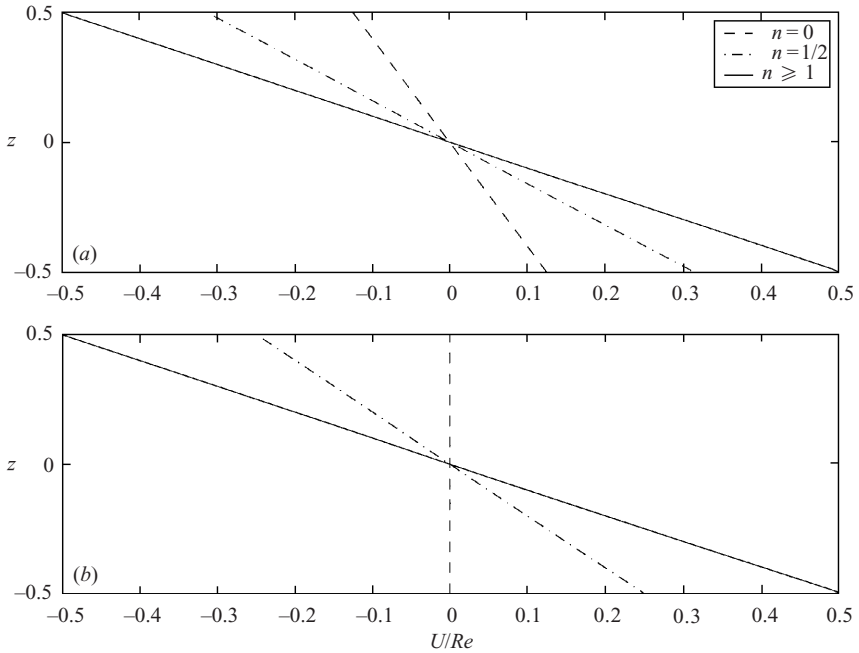


FIGURE 1. Asymptotic mean profiles of the optimal solutions in plane Couette flow for $f = DI^n$ (a) and $f = D_m I^n$ (b). In both plots, the solid line represents the laminar profile which is recovered for $f = DI^n$ with $n \geqslant 1$ and for $f = D_m I^n$ for $n \geqslant 2$; (b) shows that there is zero interior shear for $f = D_m$.

in units of ν^3/d^4 *where* ν *is the kinematic viscosity and* d *the plate separation, and* $D_{lam} = Re^2$. *The Reynolds number* Re *is based upon the plate separation and either the total velocity differential across the plates* (*PCF*) *or* $\frac{3}{2}$ *of the mean velocity* (*PPF*). *For PPF, it is conjectured that* $\mathbb{D}_{max}$ *is* $\frac{64}{27}$ *times the PCF value.*

Figures 1 and 2 show how the interior mean profiles of the optimal solutions vary as the functional maximized is changed. Practically, the hope must be that the right-hand sides of (5.1) and (5.2) also provide upper bounds on $\mathbb{D}(\mathbb{D}_v/\mathbb{D}_m)^n$ and $\mathbb{D}_m(\mathbb{D}_v/\mathbb{D}_m)^n$ respectively. As way of comparison, the standard Prandtl–von Kármán mixing length closure predicts that $\mathbb{I} = O(\log Re)$, $\mathbb{D} = \mathbb{D}_v = O(Re^3/(\log Re)^2)$ and $\mathbb{D}_m = O(Re^3/(\log Re)^3)$ for asymptotically large Re so that $\mathbb{D}(\mathbb{D}_v/\mathbb{D}_m)^n = O(Re^3(\log Re)^{n-2})$ and $\mathbb{D}_m(\mathbb{D}_v/\mathbb{D}_m)^n = O(Re^3(\log Re)^{n-3})$. Other results established in this paper are the following.

(i) For the particular family of functionals $f = \mathbb{D}g(\mathbb{I})$, it has been shown that the classical Euler–Lagrange approach of Howard–Busse and the background approach of Doering–Constantin can be derived from the same Lagrangian (see Appendix D). This means that the variational formulations are complementary and trial function estimates secured in each can then be used to bracket the true bound value. This finding extends earlier demonstrations in the context of bounding the total energy dissipation in plane Couette flow (Kerswell 1998) and heat flux in Boussinesq convection (Kerswell 2001). It now seems clear that whenever a background variational problem can be formulated, the corresponding Howard–Busse approach will yield the complementary variational problem.

(ii) An explicit demonstration is given of the intimate connection between the

https://doi.org/10.1017/S0022112002008303 Published online by Cambridge University Press

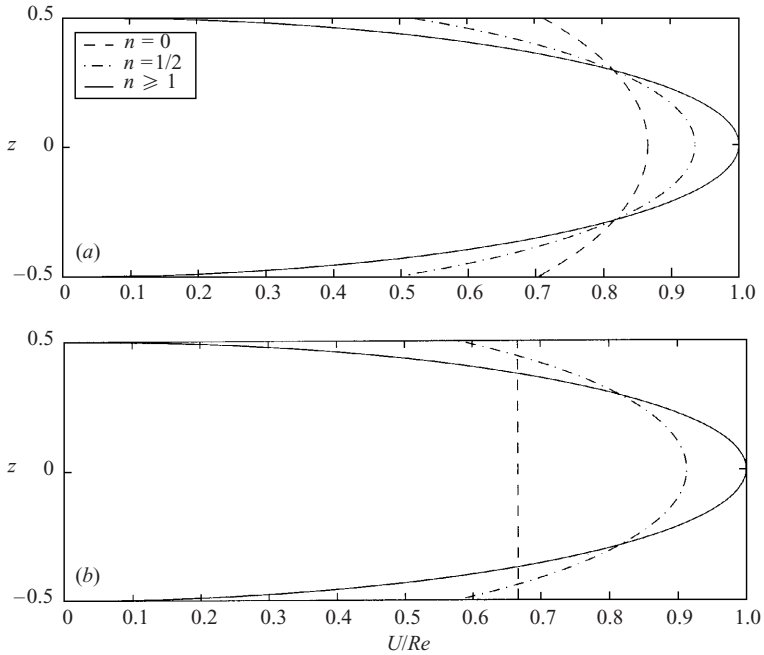


FIGURE 2. Asymptotic mean profiles of the optimal solutions in plane Poiseuille flow for $f = DI^n$ (a) and $f = D_m I^n$ (b). In both plots, the solid line represents the laminar profile which is recovered for $f = DI^n$ with $n \geqslant 1$ and for $f = D_m I^n$ for $n \geqslant 2$; (b) shows that there is zero interior shear for $f = D_m$.

background method and the classical Howard–Busse approach for bounding the total energy dissipation in plane Poiseuille flow (see Appendix C). This 'unification' (for the PCF equivalent see Kerswell 1998) is important because it provides the foundation for constructing variational problems to treat more general dissipation functionals.

(iii) The multiple-boundary-layer technique discovered by Busse has successfully been developed to treat general dissipation functionals (see Appendix A). *A priori*, it is unclear how good the ensuing bound underestimates are until comparison is made with the bound overestimate available within the complementary Doering–Constantin background method. For all functionals studied here, the multiple-boundary-layer technique is found to successfully estimate the true maximum or upper bound.

(iv) In the process of developing bounds for functionals of the form $f = D_m I^n$, we have shown how the generation of an appropriate background variational problem is not algorithmic. The 'obvious' formulation which works for $0 \leqslant n \leqslant 1$ essentially fails for $n > 1$. A formal upper bound is still available but this can never be refined to approach the true bound value by selecting improved trial functions. This is because the saddle point of the Lagrangian which represents the true bound value is no longer in the region accessible by the background technique and so the best bound estimate is only a non-optimal boundary value (see expression (4.60)). A simple reformulation (see (4.61)) however restores the duality with the Howard–Busse estimate for $n > 1$.

(v) The formal variational problem to bound the efficiency functional has been derived (see (4.28)–(4.30)) and the optimal background field related to that for the total dissipation case. The optimal efficiency background field is found to be given by the optimal total-dissipation background field after a rescaling of Re (see Appendix B). Equation (4.14) then implies that a logarithmic layer only appears in the optimal

https://doi.org/10.1017/S0022112002008303 Published online by Cambridge University Press

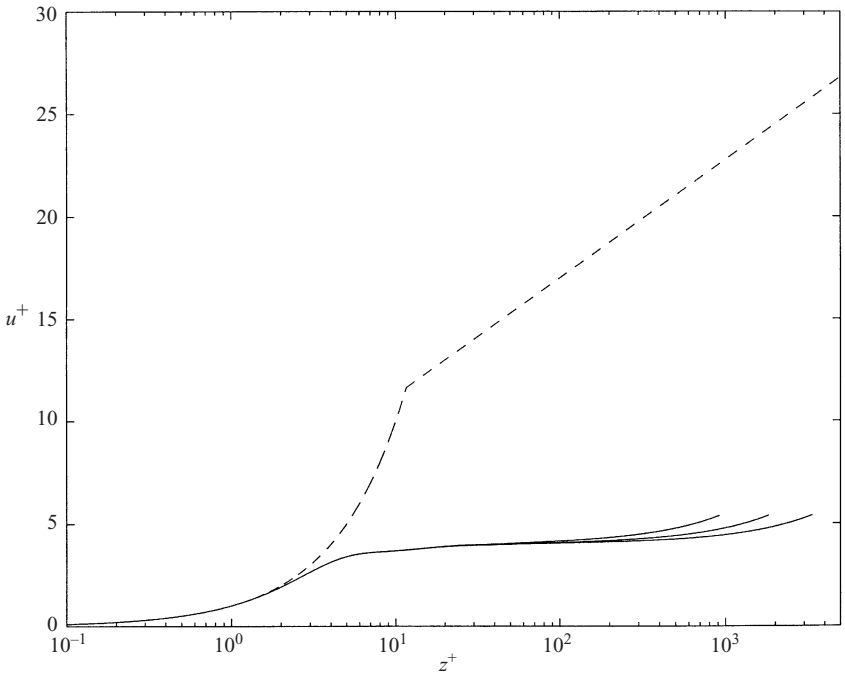


FIGURE 3. A plot of the optimal mean profiles (solid lines) which emerge from the Busse–Doering–Constantin problem (which maximizes the total dissipation $\mathbb{D}$) in friction velocity–wall units at $Re = 2 \times 10^4$, 4×10^4 and 7.33×10^4 (the larger Re, the further the mean profile reaches across the z^+-axis). Also drawn for comparison (dashed line) is the traditional fit to the data: $u^+ = z^+$ and $u^+ = 2.5 \ln z^+ + 5.5$. The plot shows the lack of any log-layer signature in the optimal mean profiles. Full details are available in Plasting & Kerswell (2002).

mean profile for the efficiency functional if it exists in the total dissipation case. This seems to contradict the findings of Malkus & Smith (1989). Recent numerical calculations aimed at solving the Busse and Doering–Constantin problem for the total dissipation in PCF *simultaneously* have found no evidence for a logarithmic layer in the mean profile (see figure 3 and Plasting & Kerswell 2002 for details). Furthermore, the asymptotic interior profiles for both PCF and PPF are found to be unrealistic in that the laminar shear is reproduced.

(vi) As noted by Malkus & Smith, the efficiency functional is clearly distinguished amongst the suite of functionals $f = DI^n$ as being marginally influenced by the dissipation ratio I. This is evident in the structure of the optimal solution which changes from $(I, D) = O(1, Re^3)$ for $0 \leqslant n < 1$ (total dissipation case is $n = 0$), through $(I, D) = O(Re^{1/3}, Re^{8/3})$ for the efficiency functional ($n = 1$) to $(I, D) = O(Re^{1/2}, Re^{5/2})$ for $n > 1$. Intriguingly, experimental data are also believed marginal in this sense with $(I, D) = O(\log Re, Re^3/(\log Re)^2)$ for large Re.

Given the generality of the analysis presented, it is straightforward to establish further results. In plane Couette flow, for example, it is currently thought that the interior mean shear will vanish as $Re \to \infty$, that is, there is no velocity defect law. The asymptotic multiple-boundary-layer analysis detailed in Appendix A for general functionals $f = f(\mathbb{D}, \mathbb{D}_m, \mathbb{D}_v)$ can be used to address the appropriate question: which functionals lead to vanishing interior shear in their optimal solutions as $Re \to \infty$? In both shear cases (see (A 53) for PPF and (A 62) for PCF) since $\mu^{1-r_N} b_1^2 \ll Re$, the

https://doi.org/10.1017/S0022112002008303 Published online by Cambridge University Press

criterion for a shearless interior is that

$$\Delta U_0 = Re\left(1 - \frac{1}{\sqrt{D_{lam}}}\frac{\gamma}{\alpha}\right). \tag{5.4}$$

Armed with the definitions (A 3) and (A 4), this reduces to

$$-\mathbb{D}_v(f_{\mathbb{D}} + f_{\mathbb{D}_v}) = 0 \quad \Rightarrow f = f(\mathbb{D} - \mathbb{D}_v, \mathbb{D}_m) = f(\mathbb{D}_m) \tag{5.5}$$

or, in other words, only a pure functional of the dissipation in the mean will lead to an asymptotically shearless interior. So if the interior shear is an important descriptor of the flow, it would seem that within the suite of functionals $f = f(\mathbb{D}, \mathbb{D}_m, \mathbb{D}_v)$ only $f = \mathbb{D}_m$ is worth studying for PCF. Conversely, this choice cannot be correct for PPF since this is believed to have a velocity defect law where the interior shear does not vanish. Hence the implication is that if a universal action functional exists, it is not contained within the suite of dissipation functionals considered here.

Of course, other aspects of the turbulent flow should be captured by the optimal variational solution beyond just the interior mean profile. In this paper, we have chosen to focus upon the ratio of the dissipations I and the total dissipation D. Within the suite of functionals $f = DI^n$, the efficiency functional has been found to be the most interesting in this respect, confirming the conclusion of Malkus & Smith (1989). However, the efficiency functional seems clearly not to be the 'action' functional if, of course, such a thing exists but nevertheless it may be close to it. Given this, it is worth examining the extended suite of functionals $f = Dg(I)$. The variational problem is as detailed in equations (4.15), (4.16) and (4.17). Working in the asymptotic limit $Re \to \infty$, and making the simplifying assumption that $D_m \gg D_{lam}I$ allows (4.17) to be rewritten as

$$f_{bound} \leqslant \frac{4a^3(a-c-1)}{27[(a-1)+(a-c-1)I]^2 c} \times \frac{g(I)^2}{g(I)'}\mathscr{D}_{max}. \tag{5.6}$$

Eliminating c by using the second consistency relation (4.16), gives

$$f_{bound} = \inf_{I,a>1} \frac{4a^3}{27(a-1)^2} \times \frac{(g(I)-g(I)'I)^2}{g(I)-(I+1)g(I)'}\mathscr{D}_{max} = \inf_{I} \frac{(g(I)-g(I)'I)^2}{g(I)-(I+1)g(I)'}\mathscr{D}_{max} \tag{5.7}$$

(the efficiency case $g = I$ has $D_m = O(D_{lam}I)$ and hence is excluded). From this it is hard to see how an optimal value of I scaling with $\log Re$ will emerge, unless $g(I)$ contains the Reynolds number in some explicit fashion. Moreover, $I \sim O(\log Re)$ will only lead to $D \sim O(Re^3/\log Re)$ rather than the observed $D \sim O(Re^3/(\log Re)^2)$ scaling of real flows. The implication of this exploratory calculation seems to be that the 'action' functional is probably not a simple functional of the dissipations.

In summary, this paper has shown how to extend some existing variational tools to treat new functionals. A first step has been to consider a family of generalized dissipation functionals motivated by previous work (Malkus & Smith 1989). The so-called 'efficiency' functional has emerged as a distinguished choice within this family but its wider importance beyond this is not clear. The challenge therefore remains to find a functional whose optimization over a tractably reduced set of dynamical constraints leads to the emergence of realistic optimal velocity fields. Unfortunately, it remains unclear how to construct such a functional beyond intelligent guessing.

https://doi.org/10.1017/S0022112002008303 Published online by Cambridge University Press

Appendix A. Multiple-boundary-layer solutions

In this Appendix we develop a solution $\boldsymbol{v}$ to the Euler–Lagrange problem (3.2) of § 3 at asymptotically large Re for general f, making only mild assumptions on the solution field. The problem to be treated in $\boldsymbol{v}$ is

$$[\alpha(\overline{uw} - h\langle huw\rangle) - \gamma h]\begin{bmatrix} w \\ 0 \\ u \end{bmatrix} + \nabla p = \nabla^2 \boldsymbol{v}, \tag{A 1}$$

$$\nabla \cdot \boldsymbol{v} = 0, \quad \boldsymbol{v}(x, y, \pm\tfrac{1}{2}) = \boldsymbol{0} \tag{A 2}$$

where

$$\alpha := \frac{(\mathbb{D} - D_{lam})f_{\mathbb{D}} + (\mathbb{D}_m - D_{lam})f_{\mathbb{D}_m} + \mathbb{D}_v f_{\mathbb{D}_v}}{(\mathbb{D} - D_{lam})f_{\mathbb{D}} + 2(\mathbb{D}_m - D_{lam})f_{\mathbb{D}_m} + (\mathbb{D}_v - \mathbb{D}_m + D_{lam})f_{\mathbb{D}_v}}, \tag{A 3}$$

$$\gamma := \tfrac{1}{2}\sqrt{D_{lam}}\,\frac{(\mathbb{D} + \mathbb{D}_m - 2D_{lam})f_{\mathbb{D}} + 2(\mathbb{D}_m - D_{lam})f_{\mathbb{D}_m} + \mathbb{D}_v f_{\mathbb{D}_v}}{(\mathbb{D} - D_{lam})f_{\mathbb{D}} + 2(\mathbb{D}_m - D_{lam})f_{\mathbb{D}_m} + (\mathbb{D}_v - \mathbb{D}_m + D_{lam})f_{\mathbb{D}_v}}, \tag{A 4}$$

and $h = h(z)$ is given (with $\langle h^2\rangle = 1$). An asymptotic solution is calculated below under the assumption that $\mu := \langle huw\rangle$ is large compared to Re, which is itself large, and that

$$\frac{\langle(\overline{uw} - h\langle huw\rangle)^2\rangle}{\langle huw\rangle^2} \ll 1. \tag{A 5}$$

The latter criterion implies that the *normalized* mean flow gradient

$$\bar{U}'(z) := \frac{U' + \sqrt{D_{lam}}h}{\langle huw\rangle} = \frac{\overline{uw} - h\langle huw\rangle}{\langle huw\rangle}$$

must have a boundary layer structure and effectively vanish in the interior. This is the physically observed case of interest and appears readily satisfied by all f studied here. The solution strategy is to construct a multiple-boundary-layer structure for $\boldsymbol{v}$ in which $\bar{U}'$ gradually relaxes from being $O(1)$ in the innermost boundary layer where $\overline{uw} = 0$ at the plates to small values in the interior where $\overline{uw} \approx h\langle huw\rangle$. This procedure was introduced by Busse (1969, 1970, 1978) to develop trial function underestimates of the maximal energy dissipation possible in convective turbulence and turbulent shear flows. The purpose here is to demonstrate the usefulness of this technique for more general variational problems addressing other functionals.

Following Busse's original work, we look for a two-dimensional solution independent of the streamwise coordinate ($\partial/\partial x = 0$)

$$\boldsymbol{v} = \nabla \times (\psi\hat{\boldsymbol{z}}) + \nabla \times \nabla \times (v\hat{\boldsymbol{z}}) = \begin{bmatrix} \psi_y \\ v_{yz} \\ -v_{yy} \end{bmatrix} = \begin{bmatrix} u \\ \cdot \\ w \end{bmatrix}. \tag{A 6}$$

Taking $\hat{\boldsymbol{z}} \cdot \nabla \times$ (A 1) and $\hat{\boldsymbol{z}} \cdot \nabla \times \nabla \times$ (A 1) gives respectively

$$[\alpha(\overline{uw} - h\langle huw\rangle) - \gamma h]w_y = \nabla^2 u_y, \tag{A 7}$$

$$[\alpha(\overline{uw} - h\langle huw\rangle) - \gamma h]u_{yy} = \nabla^4 w. \tag{A 8}$$

We search for a solution in the form of Busse's multiple-boundary-layer ansatz,

$$[u, w] = \sum_{n=1}^{N} \sqrt{2}[u_n(z), w_n(z)] \cos k_n y, \tag{A 9}$$

https://doi.org/10.1017/S0022112002008303 Published online by Cambridge University Press

where the N boundary layers are defined by the stretched coordinates

$$\xi_n := \mu^{r_n}(\tfrac{1}{2} \mp z), \tag{A 10}$$

and the wavenumbers $k_n^2 = \mu^{q_n} b_n^2$ ($b_n = O(1)$). The nth harmonic has a triple-deck structure. In the inner boundary layer deck, which defines the nth layer ($\xi_n = O(1)$), the solution is

$$[u_n(z), w_n(z)] = [\mu^{(1/2)+p_n}\hat{u}_n(\xi_n), \mu^{(1/2)-p_n}\hat{w}_n(\xi_n)] \tag{A 11}$$

so that $\hat{u}_n, \hat{w}_n = O(1)$ and the ratio of z-lengthscales to x-lengthscales is small. The solution in the intermediate deck, where the ratio of z-lengthscales to x-lengthscales is $O(1)$, makes no significant contribution to the nth harmonic dissipation and so is suppressed. The outer deck of the first harmonic ($n = 1$) coincides with the main stream ($\frac{1}{2} - |z| = O(1)$ referred to as the *zeroth* layer: $r_0 = 0$), while those for the higher harmonics ($2 \leqslant n \leqslant N$) lie in the $(n-1)$th layer and have large ratio of z-lengthscales to x-lengthscales. The outer-deck solution for the nth harmonic is

$$[u_n(z), w_n(z)] = [\mu^{(1/2)+s_n}\tilde{u}_n(\xi_{n-1}), \mu^{(1/2)-s_n}\tilde{w}_n(\xi_{n-1})], \tag{A 12}$$

where $\tilde{u}_n, \tilde{w}_n = O(1)$. The intriguing feature of Busse's multiple-boundary-layer structure is the interweaving of neighbouring harmonics so that $\overline{uw} - h\langle huw\rangle = \mu(\hat{u}_n\hat{w}_n + \tilde{u}_{n+1}\tilde{w}_{n+1} - h)$ remains close to zero in all layers except the wall boundary layer ($n = N$). Within this boundary layer approximation, equations (A 7) and (A 8) become: in the interior ($n = 0$)

$$-\mu^{1-2s_1-q_1}[\alpha(\tilde{u}_1\tilde{w}_1 - h(z)) - \gamma h(z)/\mu]\tilde{w}_1 = b_1^2\tilde{u}_1, \tag{A 13}$$

$$-\mu^{1+2s_1-q_1}[\alpha(\tilde{u}_1\tilde{w}_1 - h(z)) - \gamma h(z)/\mu]\tilde{u}_1 = b_1^2\tilde{w}_1; \tag{A 14}$$

in the nth layer ($1 \leqslant n \leqslant N-1$) near $z = \frac{1}{2}$

$$\mu^{1-2p_n-2r_n}\alpha(\hat{u}_n\hat{w}_n + \tilde{u}_{n+1}\tilde{w}_{n+1} - h_0)\hat{w}_n = \hat{u}_n'', \tag{A 15}$$

$$-\mu^{1+2p_n-4r_n+q_n}\alpha(\hat{u}_n\hat{w}_n + \tilde{u}_{n+1}\tilde{w}_{n+1} - h_0)\hat{u}_n = \hat{w}_n^{\mathrm{iv}}/b_n^2, \tag{A 16}$$

$$-\mu^{1-2s_{n+1}-q_{n+1}}\alpha(\hat{u}_n\hat{w}_n + \tilde{u}_{n+1}\tilde{w}_{n+1} - h_0)\tilde{w}_{n+1} = b_{n+1}^2\tilde{u}_{n+1}, \tag{A 17}$$

$$-\mu^{1+2s_{n+1}-q_{n+1}}\alpha(\hat{u}_n\hat{w}_n + \tilde{u}_{n+1}\tilde{w}_{n+1} - h_0)\tilde{u}_{n+1} = b_{n+1}^2\tilde{w}_{n+1}; \tag{A 18}$$

and in the innermost wall layer ($n = N$) near $z = \frac{1}{2}$

$$\mu^{1-2p_N-2r_N}\alpha(\hat{u}_N\hat{w}_N - h_0)\hat{w}_N = \hat{u}_N'', \tag{A 19}$$

$$-\mu^{1+2p_N-4r_N+q_N}\alpha(\hat{u}_N\hat{w}_N - h_0)\hat{u}_N = \hat{w}_N^{\mathrm{iv}}/b_N^2, \tag{A 20}$$

where $h_0 := h(\frac{1}{2})$. The fact that γh_0 can be ignored relative to $\alpha(\overline{uw} - h\langle huw\rangle)$ in all but the interior equations follows from the integral power relation

$$2\gamma\mu = \langle|\boldsymbol{\nabla v}|^2\rangle + 2\alpha\langle(\overline{uw} - h\langle huw\rangle)^2\rangle. \tag{A 21}$$

These boundary layer equations imply

$$\left.\begin{aligned} &-2s_1 - q_1 = 2s_1 - q_1, \quad -2p_N - 2r_N = 2p_N - 4r_N + q_N, \\ &-2p_n - 2r_n = 2p_n - 4r_n + q_n = -2s_{n+1} - q_{n+1}, \\ &-2s_{n+1} - q_{n+1} = 2s_{n+1} - q_{n+1}, \end{aligned}\right\} \quad n = 1, \ldots, N-1, \tag{A 22}$$

which indicate an equipartition of dissipations within a given boundary layer, that is, the dissipations associated with each component field ($\hat{u}_n$, $\hat{w}_n$, $\tilde{u}_{n+1}$, $\tilde{w}_{n+1}$) are all

https://doi.org/10.1017/S0022112002008303 Published online by Cambridge University Press

of the same order. Also, it follows immediately that $s_n = 0$ for $n = 1, \ldots, N$. Further implications of equations (A 15)–(A 18) are that

$$\frac{1}{b_n^2}\int_0^\infty \hat{w}_n''^2 \,\mathrm{d}\xi_n = \int_0^\infty \hat{u}_n'^2 \,\mathrm{d}\xi_n, \quad n = 1, \ldots, N, \tag{A 23}$$

$$\left.\begin{aligned} \tilde{u}_{n+1}^2 &= \tilde{w}_{n+1}^2 = h_0 - \hat{u}_n\hat{w}_n, \\ b_{n+1}^2 &= \mu^{1-q_{n+1}}\alpha(h_0 - \hat{u}_n\hat{w}_n - \tilde{u}_{n+1}\tilde{w}_{n+1}), \end{aligned}\right\} \quad n = 1, \ldots, N-1, \tag{A 24}$$

$$b_1^2 = \mu^{1-q_1}[\alpha(h - \tilde{u}_1\tilde{w}_1) + \gamma h/\mu], \tag{A 25}$$

$$\tilde{u}_1 = \tilde{w}_1 = \sqrt{h(z)}. \tag{A 26}$$

The problem for the nth harmonic is then

$$\hat{u}_n'' = -b_{n+1}^2\hat{w}_n, \quad \hat{w}_n^{\mathrm{iv}} = b_n^2 b_{n+1}^2\hat{u}_n \tag{A 27}$$

provided $\hat{u}_n\hat{w}_n$ differs from h_0, otherwise $\tilde{u}_{n+1}$ and $\tilde{w}_{n+1}$ vanish. In the region where $\hat{u}_n\hat{w}_n = h_0$, (A 16) can be rewritten as

$$\frac{1}{b_n^2}\hat{w}_n^{\mathrm{iv}} = \frac{\hat{w}_n''\hat{w}_n - 2\hat{w}_n'^2}{\hat{w}_n^5}h_0^2. \tag{A 28}$$

In the region described by this equation w_n has to tend to infinity in order to join $\mu^{p_n}\tilde{w}_n$ while $\hat{w}_n''$ and $\hat{w}''''_n$ have to tend to zero in order to yield finite values for the dissipation integrals. This condition together with the condition $\hat{w}_n = \hat{w}_n' = \hat{u}_n = 0$ at $\xi_n = 0$ suffices to determine the solution of (A 27) and (A 28). Busse (1969*a*) has solved this problem and it suffices here only to note that

$$\int_0^\infty \left(\frac{\hat{w}_n''^2}{b_n^2} + b_{n+1}^2\tilde{w}_{n+1}^2\right)\mathrm{d}\xi_n = 3\beta h_0\left(\frac{b_{n+1}^4}{b_n}\right)^{1/3} \tag{A 29}$$

for $n = 1, \ldots, N-1$ where $\beta \approx 0.624$. In the interior

$$b_1^2\langle\tilde{u}_1^2\rangle = b_1^2\langle\tilde{w}_1^2\rangle = h_0 h_1 b_1^2, \tag{A 30}$$

where $h_1 = \langle|h(z)|\rangle/h_0$. In the innermost layer, $h_0 - \hat{u}_N\hat{w}_N = O(1)$ so that

$$\alpha = O(\mu^a = \mu^{2p_N + 2r_N - 1}). \tag{A 31}$$

With this realization, write $\alpha = \mu^a\hat{\alpha}$ ($\hat{\alpha} = O(1)$), and then a change of variable,

$$\Omega = \hat{w}_N b_N^{-1/3}(\hat{\alpha}h_0)^{1/6}h_0^{-1/2}, \quad \Theta = \hat{u}_N b_N^{1/3}(\hat{\alpha}h_0)^{-1/6}h_0^{-1/2}, \quad x = \xi_N b_N^{1/3}(\hat{\alpha}h_0)^{1/3}, \tag{A 32}$$

reduces the innermost boundary layer equations to

$$[1 - \Theta\Omega]\Theta = \Omega^{\mathrm{iv}}, \tag{A 33}$$

$$-[1 - \Theta\Omega]\Omega = \Theta''. \tag{A 34}$$

These together with the corresponding boundary conditions have been solved by Howard (1963) with the result that

$$\int_0^\infty \frac{\hat{w}_N''^2}{b_N^2}\,\mathrm{d}\xi_N = \int_0^\infty \hat{u}_N'^2\,\mathrm{d}\xi_N = \frac{\sigma h_0(\hat{\alpha}h_0)^{2/3}}{b_N^{1/3}}, \quad \int_0^\infty (h_0 - \hat{u}_N\hat{w}_N)^2\,\mathrm{d}\xi_N = \frac{4\sigma h_0^2}{(\hat{\alpha}h_0)^{1/3}b_N^{1/3}}, \tag{A 35}$$

https://doi.org/10.1017/S0022112002008303 Published online by Cambridge University Press

where $\sigma \approx 0.337$. Within this boundary layer approximation,

$$\begin{aligned}\mathbb{D}_v &= \langle|\nabla \boldsymbol{v}|^2\rangle = \langle(\nabla^2 v_y)^2\rangle + \langle|\nabla u|^2\rangle \\ &\approx \left\{2\sum_{n=1}^{N}\mu^{1-2p_n+3r_n-q_n}\int_0^\infty \frac{\hat{w}_n''^2}{b_n^2}\,\mathrm{d}\xi_n + 2\sum_{n=1}^{N-1}\mu^{1+q_{n+1}-r_n}\int_0^\infty b_{n+1}^2\tilde{w}_{n+1}^2\,\mathrm{d}\xi_n\right\} + \mu^{1+q_1}b_1^2\langle\tilde{w}_1^2\rangle \\ &\quad + \left\{2\sum_{n=1}^{N}\mu^{1+2p_n+r_n}\int_0^\infty \hat{u}_n'^2\,\mathrm{d}\xi_n + 2\sum_{n=1}^{N-1}\mu^{1+q_{n+1}-r_n}\int_0^\infty b_{n+1}^2\tilde{u}_{n+1}^2\,\mathrm{d}\xi_n\right\} + \mu^{1+q_1}b_1^2\langle\tilde{u}_1^2\rangle, \\ &\approx 2\mu^{1+q_1}h_0h_1b_1^2 + 12\beta h_0\sum_{n=1}^{N-1}\mu^{1+q_{n+1}-r_n}\left(\frac{b_{n+1}^4}{b_n}\right)^{1/3} + \mu^{2-r_N+a}\frac{4\sigma h_0(\hat{\alpha}h_0)^{2/3}}{b_N^{1/3}}, \end{aligned} \tag{A 36}$$

$$\begin{aligned}\mathbb{D}_m - D_{lam} = \langle(\overline{uw} - h\langle huw\rangle)^2\rangle &\approx 2\mu^{2-r_N}\int_0^\infty(\hat{u}_N\hat{w}_N - h_0)^2\,\mathrm{d}\xi_N, \\ &\approx \mu^{2-r_N}\frac{8\sigma h_0^2}{(\hat{\alpha}h_0)^{1/3}b_N^{1/3}}\end{aligned} \tag{A 37}$$

(it can be shown *a posteriori* that the contribution from the innermost layer to the dissipation in the mean dominates all others), and

$$\mathbb{D} = D_{lam} + \sqrt{D_{lam}}\mu. \tag{A 38}$$

The problem of extremizing $\mathscr{L}$ in (3.1) over $\boldsymbol{v}$ has been transformed into the problem of extremizing L over the multiple-boundary-layer wavenumbers $\boldsymbol{b} = (b_1, b_2, \ldots, b_N)$ and μ. The Euler–Lagrange equations are

$$(f_{\mathbb{D}_v} + \Lambda)\left.\frac{\partial \mathbb{D}_v}{\partial b_n}\right|_\mu = 0, \quad n = 1, \ldots, N-1, \tag{A 39}$$

$$\alpha\left.\frac{\partial \mathbb{D}_m}{\partial b_N}\right|_\mu + \left.\frac{\partial \mathbb{D}_v}{\partial b_N}\right|_\mu = 0, \tag{A 40}$$

$$(f_{\mathbb{D}} - \Lambda)\left.\frac{\partial \mathbb{D}}{\partial \mu}\right|_{\boldsymbol{b}} + (f_{\mathbb{D}_m} + \Lambda)\left.\frac{\partial \mathbb{D}_m}{\partial \mu}\right|_{\boldsymbol{b}} + (f_{\mathbb{D}_v} + \Lambda)\left.\frac{\partial \mathbb{D}_v}{\partial \mu}\right|_{\boldsymbol{b}} = 0, \tag{A 41}$$

$$\mathbb{D} - \mathbb{D}_m - \mathbb{D}_v = 0. \tag{A 42}$$

Equations (A 39) and (A 40) define the optimal wavenumbers through the relations

$$\mu^{1+q_1}h_1b_1 - \beta\mu^{1+q_2-r_1}\left(\frac{b_2}{b_1}\right)^{4/3} = 0, \tag{A 43}$$

$$4\mu^{1+q_n-r_{n-1}}\left(\frac{b_n^4}{b_{n-1}}\right)^{1/3} - \mu^{1+q_{n+1}-r_n}\left(\frac{b_{n+1}^4}{b_n}\right)^{1/3} = 0, \quad n = 2, \ldots, N-1, \tag{A 44}$$

$$\mu^{2-r_N+a}\frac{\sigma(\hat{\alpha}h_0)^{2/3}}{b_N^{4/3}} - \mu^{1+q_N-r_{N-1}}4\beta\left(\frac{b_N}{b_{N-1}}\right)^{1/3} = 0, \tag{A 45}$$

which only depend on f through α. For finite solutions, the scaling relations

$$1 + q_n - r_{n-1} = 1 + q_{n+1} - r_n, \quad n = 1, \ldots, N, \tag{A 46}$$

must hold ($q_{N+1} = 1 + a$) which imply that each boundary layer contributes at equal order to the dissipation in the fluctuation field. The optimizing wavenumbers then

https://doi.org/10.1017/S0022112002008303 Published online by Cambridge University Press

follow as

$$b_1 = \left\{ \left(\frac{\sigma}{\beta}\right)^{3/4} (\hat{\alpha} h_0)^{1/2} 4^{-N} \left[\frac{4^{4/3}\beta}{h_1}\right]^{1-4^{-N}} \right\}^{1/(2-4^{-N})}, \tag{A 47}$$

$$b_{n+1} = 4^n b_1 \left(\frac{h_1 b_1}{4^{4/3}\beta}\right)^{1-4^{-n}}, \quad \frac{b_{n+1}^{4/3}}{b_n^{1/3}} = 4^{n-1} h_1 b_1^2/\beta, \quad n = 1, \ldots, N-1. \tag{A 48}$$

Together with (A 22), (A 46) leads to the scalings

$$r_n = (1+a)\frac{1-4^{-n}}{2-4^{-N}}, \quad 2p_n = (1+a)\frac{4^{-n}}{2-4^{-N}}, \quad q_n = (1+a)\frac{2-4^{-n+1}}{2-4^{-N}}, \quad s_n = 0. \tag{A 49}$$

Then

$$\mathbb{D}_v = 2\mu^{2+a-r_N} h_0 h_1 b_1^2 (4^N - 1), \quad \mathbb{D}_m = D_{lam} + 2\mu^{2-r_N} h_0 h_1 b_1^2 \frac{4^N}{\hat{\alpha}} \tag{A 50}$$

and (A 42) becomes

$$\tfrac{1}{2}\sqrt{D_{lam}} = \mu^{1-r_N} h_0 h_1 b_1^2 \left[\mu^a (4^N - 1) + \frac{4^N}{\hat{\alpha}}\right]. \tag{A 51}$$

Equation (A 41) reproduces (3.5) so that

$$\alpha := \frac{(\mathbb{D} - D_{lam}) f_{\mathbb{D}} + (\mathbb{D}_m - D_{lam}) f_{\mathbb{D}_m} + \mathbb{D}_v f_{\mathbb{D}_v}}{(\mathbb{D} - D_{lam}) f_{\mathbb{D}} + 2(\mathbb{D}_m - D_{lam}) f_{\mathbb{D}_m} + (\mathbb{D}_v - \mathbb{D}_m + D_{lam}) f_{\mathbb{D}_v}}. \tag{A 52}$$

The solution procedure consists of finding $\alpha = \hat{\alpha}\mu^a$ from (A 52), b_1 from (A 47) and finally μ in terms of Re from (A 51) which then allows $\mathbb{D}$, $\mathbb{D}_v$, $\mathbb{D}_m$ and hence f to be expressed in terms of known constants and Re.

One of the interesting outcomes of this calculation is the mean flow profile of the optimal solution. This can be compared directly with observations and gives an immediate indication of how important dissipation in the mean is to the functional under consideration.

Mean profile for plane Poiseuille flow

The change in mean flow across half the interior ($z \in [0, \frac{1}{2}]$) from $z = \frac{1}{2}$ into the mid-plane is

$$\begin{aligned}\Delta U_0 = -\int_0^{1/2} U' \,\mathrm{d}z &= -\int_0^{1/2} (\overline{uw} - h\langle huw\rangle - 8Re\, z)\,\mathrm{d}z \\ &= \mu \int_0^{1/2} (h - \tilde{u}_1 \tilde{w}_1)\,\mathrm{d}z + Re = Re - h_0 h_1 \frac{\gamma}{2\alpha} + \mu^{1-r_N} \frac{b_1^2}{2\hat{\alpha}},\end{aligned} \tag{A 53}$$

since $b_1^2 = 2\mu^{r_N}\hat{\alpha}\int_0^{1/2}(h - \tilde{u}_1\tilde{w}_1)\,\mathrm{d}z + \mu^{-q_1} h_0 h_1 \gamma$. The corresponding change across any boundary layer except the innermost near $z = \frac{1}{2}$ is

$$\begin{aligned}\Delta U_n &= \mu^{1-r_n} \int_0^{\infty} (h_0 - \hat{u}_n \hat{w}_n - \tilde{u}_{n+1}\tilde{w}_{n+1})\,\mathrm{d}\xi_n, \\ &= \frac{\mu^{1-r_N}}{\hat{\alpha}} \int_0^{\infty} \left(\frac{\hat{w}'^2}{b_n^2} + b_{n+1}^2 \tilde{w}_{n+1}^2\right) \mathrm{d}\xi_n = \mu^{1-r_N} h_1 \frac{b_1^2}{\hat{\alpha}} 3 \times 4^{n-1}\end{aligned} \tag{A 54}$$

https://doi.org/10.1017/S0022112002008303 Published online by Cambridge University Press

so that the total change across the first $(N-1)$th boundary layer is

$$\sum_{n=1}^{N-1}\Delta U_n = 3\mu^{1-r_N}h_1\frac{b_1^2}{\hat{\alpha}}\sum_{n=1}^{N-1}4^{n-1} = \mu^{1-r_N}h_1\frac{b_1^2}{\hat{\alpha}}(4^{N-1}-1). \tag{A 55}$$

Across the innermost layer, the mean flow change is

$$\Delta U_N = \mu^{1-r_N}\int_0^\infty (h_0-\hat{u}_N\hat{w}_N)\,\mathrm{d}\xi_N = \frac{\mu^{1-r_N}h_0}{b_N^{1/3}(\hat{\alpha}h_0)^{1/3}}\left\{\int_0^\infty(1-\Omega\Theta)\,\mathrm{d}x = 5\sigma\right\},$$
$$= \mu^{1-r_N}h_1\frac{b_1^2}{\hat{\alpha}}5\times 4^{N-1}. \tag{A 56}$$

The condition of mass flux conservation,

$$\langle U\rangle = \tfrac{2}{3}Re = 2\int_0^{1/2}(z(h-\tilde{u}_1\tilde{w}_1)+8Re\,z^2)\,\mathrm{d}z + \sum_{n=1}^{N-1}\Delta U_n + \Delta U_N, \tag{A 57}$$

automatically follows from the implied power balance $2\gamma\mu = 2\alpha\langle(\overline{uw}-h\langle huw\rangle)^2\rangle + \langle|\nabla\boldsymbol{v}|^2\rangle$. As an example, set $f=\mathbb{D}$, then $\alpha=\hat{\alpha}=1$ $(a=0)$,

$$\Lambda = -\frac{\mathbb{D}}{\mathbb{D}_m}\approx -2+4^{-N},\quad \gamma = \frac{3-4^{-N}}{2-4^{-N}}\frac{2Re}{\sqrt{3}} \tag{A 58}$$

(ignoring the laminar mean dissipation, $O(Re^2)$, relative to the turbulent dissipation in the mean, $O(\mu^{2-r_N})$) and (A 51) becomes

$$\mu^{1-r_N}b_1^2 = \frac{4Re}{3(2\times 4^N-1)}. \tag{A 59}$$

Then

$$\left[\Delta U_0, \sum_{n=1}^{N-1}\Delta U_n, \Delta U_N\right] \quad\Rightarrow\quad \left[\tfrac{1}{4}Re, \tfrac{1}{12}Re, \tfrac{5}{12}Re\right] \quad \text{as} \quad Re\to\infty. \tag{A 60}$$

This means that the predicted asymptotic mean profile has the form

$$U_0 = \tfrac{3}{4}Re(1-\tfrac{1}{3}z^2)\hat{\boldsymbol{x}} \tag{A 61}$$

so that it joins the boundary at 2/3 of its maximal value at the channel centre (Busse 1970, p. 237).

Mean profile for plane Couette flow

In the case of PCF where $\boldsymbol{u}(x,y,\pm\frac{1}{2}) = \mp\frac{1}{2}Re$, $h=h_0=h_1=1$, the changes in the mean flow across half the interior, the first $(N-1)$th boundary layer and the innermost boundary layer going from the upper plate $z=\frac{1}{2}$ to the channel centre $z=0$ are

$$\Delta U_0 = \tfrac{1}{2}\left(Re - \frac{\gamma}{\alpha} + \mu^{1-r_N}\frac{b_1^2}{\hat{\alpha}}\right), \tag{A 62}$$

$$\sum_{n=1}^{N-1}\Delta U_n = \mu^{1-r_N}\frac{b_1^2}{\hat{\alpha}}(4^{N-1}-1),$$

$$\Delta U_N = \mu^{1-r_N}\frac{b_1^2}{\hat{\alpha}}5\times 4^{N-1}. \tag{A 63}$$

https://doi.org/10.1017/S0022112002008303 Published online by Cambridge University Press

The implicit power balance relation $2\gamma\mu = 2\alpha\langle(\overline{uw} - h\langle huw\rangle)^2\rangle + \langle|\nabla \boldsymbol{v}|^2\rangle$ ensures that the velocity drop across the half-layer is consistent,

$$\Delta U_0 + \sum_{n=1}^{N-1} \Delta U_n + \Delta U_N = \tfrac{1}{2} Re. \tag{A 64}$$

Again taking $f = \mathbb{D}$ as an example, then $\alpha = \hat{\alpha} = 1$ ($a = 0$),

$$\Lambda = -\frac{\mathbb{D}}{\mathbb{D}_m} \approx -2 + 4^{-N}, \quad \gamma = \frac{3 - 4^{-N}}{2 - 4^{-N}} \frac{Re}{2}, \quad \mu^{1-r_N} b_1^2 = \frac{Re}{2(2 \times 4^N - 1)}, \tag{A 65}$$

so that

$$\left[\Delta U_0, \sum_{n=1}^{N-1} \Delta U_n, \Delta U_N\right] \quad \Rightarrow \quad [\tfrac{1}{8} Re, \tfrac{1}{16} Re, \tfrac{5}{16} Re] \quad \text{as} \quad Re \to \infty. \tag{A 66}$$

This means that the predicted asymptotic mean profile has the form

$$U_0 = -\tfrac{1}{4} Re\, \hat{\boldsymbol{x}}. \tag{A 67}$$

If $f = \mathbb{D}_m$, then $\Lambda = -2$, $\alpha = \hat{\alpha} = 1/2$, $a = 0$, $\gamma = Re/2$, $\mu^{1-r_N} b_1^2 = Re/(2(3 \times 4^N - 1))$ and

$$\left.\begin{gathered} \mathbb{D}_v = 2\mu^{2-r_N} b_1^2 (4^N - 1), \quad \mathbb{D}_m = Re^2 + \mu^{2-r_N} b_1^2 4 \times 4^N, \\ \mathbb{D} = Re^2 + 2\mu^{2-r_N} b_1^2 (3 \times 4^N - 1). \end{gathered}\right\} \tag{A 68}$$

Then

$$\left[\Delta U_0, \sum_{n=1}^{N-1} \Delta U_n, \Delta U_N\right] \quad \Rightarrow \quad [0, \tfrac{1}{12} Re, \tfrac{5}{12} Re] \quad \text{as} \quad Re \to \infty. \tag{A 69}$$

This means that the predicted asymptotic mean profile has zero shear across the interior. Finally if $f = \mathbb{D}_v$, then $\Lambda = -2$, $\alpha = \hat{\alpha} = 2$, $a = 0$, $\gamma = Re$, $\mu^{1-r_N} b_1^2 = Re/(3 \times 4^N - 2)$ and

$$\mathbb{D}_v = 2\mu^{2-r_N} b_1^2 (4^N - 1), \quad \mathbb{D}_m = Re^2 + \mu^{2-r_N} b_1^2 4^N, \quad \mathbb{D} = Re^2 + \mu^{2-r_N} b_1^2 (3 \times 4^N - 2). \tag{A 70}$$

Then

$$\left[\Delta U_0, \sum_{n=1}^{N-1} \Delta U_n, \Delta U_N\right] \quad \Rightarrow \quad [\tfrac{1}{4} Re, \tfrac{1}{24} Re, \tfrac{5}{24} Re] \quad \text{as} \quad Re \to \infty. \tag{A 71}$$

This means that the predicted asymptotic mean profile has a $\frac{1}{2}$-shear law across the interior.

Appendix B

B.1. *Plane Couette flow*

Nicodemus *et al.* (1998*a*, *b*) have considered the problem of evaluating

$$\lambda := \inf_{\Phi, \hat{a} > 1} \frac{\hat{a}^2}{4(\hat{a} - 1)\widehat{Re}} \|\Phi' + 1\|_2^2 \tag{B 1}$$

over all functions $\Phi = \Phi(z)$ and scalars $\hat{a} > 1$ which satisfy the spectral constraint

https://doi.org/10.1017/S0022112002008303 Published online by Cambridge University Press

that

$$\|\nabla\hat{\boldsymbol{v}}\|_2^2 + \frac{\hat{a}\widehat{Re}}{\hat{a}-1}\langle\Phi'\hat{v}_1\hat{v}_3\rangle \geqslant 0 \tag{B 2}$$

for any incompressible $\hat{\boldsymbol{v}}$ which vanish on the boundaries $z = \pm\frac{1}{2}$ and

$$\int_{-1/2}^{1/2} \Phi'\,\mathrm{d}z = -1. \tag{B 3}$$

Through the use of a sophisticated trial function, they were able to estimate this infimum, $\lambda = \lambda(\widehat{Re})$, finding in particular that

$$\lambda \to 0.01087, \quad \hat{a} \to 3 \quad \text{as} \quad \widehat{Re} \to \infty. \tag{B 4}$$

Given their solution, $(\lambda(\widehat{Re}), \hat{a}(\widehat{Re}))$, we then know for all Φ satisfying

$$\|\nabla\hat{\boldsymbol{v}}\|_2^2 + \hat{\mu}\langle\Phi'\hat{v}_1\hat{v}_3\rangle \geqslant 0, \quad \int_{-1/2}^{1/2} \Phi'\,\mathrm{d}z = -1, \tag{B 5}$$

that

$$\inf_{\Phi} \|\Phi' + 1\|_2^2 = \frac{4(\hat{a}(\widehat{Re})-1)^2}{\hat{a}(\widehat{Re})^3}\hat{\mu}\lambda(\widehat{Re}), \tag{B 6}$$

where $\hat{\mu} := \hat{a}\widehat{Re}/(\hat{a}-1)$. In particular,

$$\inf_{\Phi} \|\Phi' + 1\|_2^2 \to \tfrac{16}{27} \times 0.01087 \times \hat{\mu} \quad \text{as} \quad \widehat{Re} \to \infty. \tag{B 7}$$

In the main body of the text, the problem for the background field is exactly given by (B 5) and (B 6) once the association $\hat{\mu} = \hat{a}\widehat{Re}/(\hat{a}-1) = aRe/c$ is made ($\phi = Re\Phi$). This means that the required background field at Re is given by the background field found by Nicodemus *et al.* (1998*a*, *b*) at the different Reynolds number $\widehat{Re}$.

We now state the result required for the main body of the text. If the background field is rescaled, $\phi := Re\,\Phi$, then (B 7) means that for all ϕ such that

$$\|\nabla\hat{\boldsymbol{v}}\|_2^2 + \mu\langle\phi'\hat{v}_1\hat{v}_3\rangle \geqslant 0, \quad \int_{-1/2}^{1/2} \phi'\,\mathrm{d}z = -Re, \tag{B 8}$$

then

$$\inf_{\phi} \|\phi' + Re\|_2^2 \to \tfrac{16}{27}\mu \times \mathscr{D}_{max}^{PCF} \quad \text{as} \quad Re \to \infty \tag{B 9}$$

where $\mathscr{D}_{max}^{PCF} := 0.01087Re^3$.

B.2. *Plane Poiseuille flow*

The Doering–Constantin problem for bounding the total dissipation in PPF is (see Appendix C)

$$\mathscr{D} := \inf_{\phi,\hat{a}>1} \frac{\hat{a}^2}{4(\hat{a}-1)}\|\phi' + 8\widehat{Re}\,z\|_2^2 \tag{B 10}$$

over all scalars $\hat{a} > 1$ and functions $\phi = \phi(z)$, where $\phi(\pm\frac{1}{2}) = 0$ and $\langle\phi\rangle = \frac{2}{3}\widehat{Re}$ which also satisfy the spectral constraint that

$$\|\nabla\hat{\boldsymbol{v}}\|_2^2 + \frac{\hat{a}}{\hat{a}-1}\langle\phi'\hat{v}_1\hat{v}_3\rangle \geqslant 0 \tag{B 11}$$

https://doi.org/10.1017/S0022112002008303 Published online by Cambridge University Press

for any incompressible $\hat{\boldsymbol{v}}$, where $\hat{\boldsymbol{v}}(x, y, \pm\frac{1}{2}) = \boldsymbol{0}$. Although this problem has not been solved, there is enough similarity with the corresponding PCF problem to reasonably speculate that

$$\mathscr{D} \to \tfrac{64}{27} \times 0.01087\widehat{Re}^3, \quad \hat{a} \to 3 \quad \text{as} \quad \widehat{Re} \to \infty. \tag{B 12}$$

The factor $\frac{64}{27}$ comes from the ratio of dissipation bounds produced by Busse in PPF and PCF. That $\hat{a}$ should have the same limiting value is suggested by the optimal solution in the PCF problem where ϕ develops two boundary layers and very little structure in the interior at large Re. In the PPF problem, the same boundary layer structure should emerge but now organized symmetrically about the mid-plane.

By reasoning similar to that used above in § B.1, and modulo the assumption (B 12) we can conclude that for all ϕ such that

$$\|\nabla\hat{\boldsymbol{v}}\|_2^2 + \mu\langle\phi'\hat{v}_1\hat{v}_3\rangle \geqslant 0, \quad \int_{-1/2}^{1/2} \phi \,\mathrm{d}z = \tfrac{2}{3}Re, \quad \phi(\pm\tfrac{1}{2}) = 0, \tag{B 13}$$

then

$$\inf_{\phi} \|\phi' + 8Re\, z\|_2^2 \to \tfrac{16}{27}\mu \times \mathscr{D}_{max}^{PPF} \quad \text{as} \quad Re \to \infty \tag{B 14}$$

where $\mathscr{D}_{max}^{PPF} := \frac{64}{27} \times 0.01087Re^3$.

Appendix C

Here we demonstrate how the Doering–Constantin formulation for putting an upper bound on the energy dissipation in constant-mass-flux plane Poiseuille flow may be derived from the same functional as Busse's (1970) upper bounding problem. Doering & Constantin originally looked at *lower* bounding the energy dissipation in constant-pressure-gradient plane Poiseuille flow (Constantin & Doering 1995).

Using the non-dimensionalization described in § 2.2, the starting point is the functional

$$\mathscr{L} = \limsup_{T\to\infty} \frac{1}{T} \int_0^T \mathrm{d}t\{\langle|\nabla\boldsymbol{u}|^2\rangle - \langle a\boldsymbol{v}\cdot(NS)\rangle + \lambda\langle\tfrac{2}{3}Re - \boldsymbol{u}\cdot\hat{\boldsymbol{x}}\rangle\}, \tag{C 1}$$

where

$$(NS) := \frac{\partial\boldsymbol{u}}{\partial t} + \boldsymbol{u}\cdot\nabla\boldsymbol{u} + \nabla p - A\hat{\boldsymbol{x}} - \nabla^2\boldsymbol{u}. \tag{C 2}$$

The Lagrange multiplier fields $\boldsymbol{v}$ and λ impose the Navier–Stokes equations and the definition of the Reynolds number as constraints. Setting $\boldsymbol{u}(\boldsymbol{x}, t) = \phi(z)\hat{\boldsymbol{x}} + \boldsymbol{v}(\boldsymbol{x}, t)$ with $\langle\boldsymbol{v}\rangle = \boldsymbol{0}$ and boundary conditions $\phi(\pm\frac{1}{2}) = v_i(x, y, \pm\frac{1}{2}) = 0$ means that $\mathscr{L}$ can be rewritten as

$$\mathscr{L} = \langle\phi'^2\rangle + \lambda\langle\tfrac{2}{3}Re - \phi\rangle - \limsup_{T\to\infty} \frac{1}{T} \int_0^T \mathrm{d}t\langle(a-1)|\nabla\boldsymbol{v}|^2 + av_1v_3\phi' - (a-2)\phi''v_1 - \mu v_1\rangle, \tag{C 3}$$

where μ is the Lagrange multiplier which now imposes $\langle v_1\rangle = 0$ ($\langle v_2\rangle = \langle v_3\rangle = 0$ are forced by the boundary conditions). The Doering–Constantin and Busse variational problems stem from realizing that the stationary point(s) of $\mathscr{L}$ occur for steady $\boldsymbol{v}$ or equivalently coincide with the stationary point(s) of

$$D = \langle\phi'^2\rangle + \lambda\langle\tfrac{2}{3}Re - \phi\rangle - \langle(a-1)|\nabla\boldsymbol{v}|^2 + av_1v_3\phi' - (a-2)\phi''v_1 - \mu v_1\rangle. \tag{C 4}$$

https://doi.org/10.1017/S0022112002008303 Published online by Cambridge University Press

Therefore the full set of Euler–Lagrange equations which must be solved at fixed Re (constant mass flux) is

$$\frac{\delta D}{\delta \phi} = -2\phi'' - \lambda + a\overline{v_1 v_3}' + (a-2)\bar{v}_1'' = 0, \tag{C 5}$$

$$\frac{\delta D}{\delta a} = \langle |\nabla \boldsymbol{v}|^2 + v_1 v_3 \phi' - \phi'' v_1 \rangle = 0, \tag{C 6}$$

$$\frac{\delta D}{\delta \lambda} = \tfrac{2}{3} Re - \langle \phi \rangle = 0, \tag{C 7}$$

$$\frac{\delta D}{\delta \mu} = \langle v_1 \rangle = 0, \tag{C 8}$$

$$\frac{\delta D}{\delta \boldsymbol{v}} = 2(a-1)\nabla^2 \boldsymbol{v} - a\phi' \begin{bmatrix} v_3 \\ 0 \\ v_1 \end{bmatrix} + \nabla p + [(a-2)\phi'' + \mu]\hat{\boldsymbol{x}} = \boldsymbol{0}. \tag{C 9}$$

If the fluctuation field $\boldsymbol{v}$ is split into a mean part $\bar{v}_1(z)\hat{\boldsymbol{x}}$ and a part with no mean, $\hat{\boldsymbol{v}}$ ($\overline{\hat{\boldsymbol{v}}} = \boldsymbol{0}$), the last equation splits into two, namely

$$\frac{\delta D}{\delta \hat{\boldsymbol{v}}} = 2(a-1)\nabla^2 \hat{\boldsymbol{v}} - a\phi' \begin{bmatrix} \hat{v}_3 \\ 0 \\ \hat{v}_1 \end{bmatrix} + \nabla \hat{p} = \boldsymbol{0}, \tag{C 10}$$

$$\frac{\delta D}{\delta \bar{v}_1} = 2(a-1)\bar{v}_1'' + (a-2)\phi'' + \mu = 0. \tag{C 11}$$

The Doering–Constantin problem is the variational problem left in ϕ and a if the variational equations

$$\frac{\delta D}{\delta \lambda} = \frac{\delta D}{\delta \mu} = \frac{\delta D}{\delta \bar{v}_1} = 0, \quad \frac{\delta D}{\delta \hat{\boldsymbol{v}}} = \boldsymbol{0} \tag{C 12}$$

are solved. In contrast, the Busse problem is the variational problem left in $\hat{\boldsymbol{v}}$ if the variational equations

$$\frac{\delta D}{\delta \phi} = \frac{\delta D}{\delta a} = \frac{\delta D}{\delta \lambda} = \frac{\delta D}{\delta \mu} = \frac{\delta D}{\delta \bar{v}_1} = 0 \tag{C 13}$$

are solved.

C.1. *Doering–Constantin problem*

Solving (C 11) and (C 8) using (C 7) gives

$$\bar{v}_1 = -\frac{a-2}{2(a-1)}[\phi - Re(1-4z^2)]. \tag{C 14}$$

Then exploiting the fact that $\langle \bar{v}_1 \, \delta D/\delta \bar{v}_1 \rangle = 0$ to rewrite D gives

$$D = \frac{a^2}{4(a-1)} \langle (\phi' + 8Re\, z \rangle + \mathbb{D}_{lam} - \hat{\mathscr{G}}(a, \phi, \hat{\boldsymbol{v}}), \tag{C 15}$$

where $\mathbb{D}_{lam} = \langle (8Re\, z)^2 \rangle$ and

$$\hat{\mathscr{G}}(a, \phi, \hat{\boldsymbol{v}}) := (a-1)\langle |\nabla \hat{\boldsymbol{v}}|^2 \rangle + a\langle \hat{v}_1 \hat{v}_3 \phi' \rangle. \tag{C 16}$$

https://doi.org/10.1017/S0022112002008303 Published online by Cambridge University Press

As $\hat{\mathscr{G}}$ is homogeneous in $\hat{\boldsymbol{v}}$, if $\inf_{\hat{\boldsymbol{v}}} \hat{\mathscr{G}}$ exists (which is a condition on ϕ) it is 0 so that the Doering–Constantin upper bound on the long-time-averaged dissipation rate is

$$\inf_{a>1,\phi} \frac{a^2}{4(a-1)} \langle (\phi' + 8Re\, z)^2 \rangle + \mathbb{D}_{lam} \tag{C 17}$$

for ϕ which satisfies $\phi(\pm\frac{1}{2}) = 0$, $\langle \phi \rangle = \frac{2}{3}Re$, and the so-called spectral constraint that

$$\hat{\mathscr{G}} \geqslant 0 \quad \forall\, \hat{\boldsymbol{v}} \quad \text{with} \quad \boldsymbol{\nabla} \cdot \hat{\boldsymbol{v}} = 0,\ \hat{\boldsymbol{v}}(x, y, \pm\tfrac{1}{2}) = \boldsymbol{0}. \tag{C 18}$$

Finding the $\hat{\boldsymbol{v}}$ which attains $\inf_{\hat{\boldsymbol{v}}} \hat{\mathscr{G}} = 0$ corresponds to solving $\delta D/\delta \hat{\boldsymbol{v}} = \boldsymbol{0}$.

C.2. *Busse problem*

Solving (C 11), (C 8), (C 7) and (C 5) leads to (C 14) and

$$\phi' + 8Re\, z = \frac{2(a-1)}{a} (\overline{\hat{v}_1 \hat{v}_3} - h\langle h \hat{v}_1 \hat{v}_3 \rangle), \tag{C 19}$$

where $h = \sqrt{12}z$, and if the mean profile is to be symmetric about the mid-plane, $\langle \hat{v}_1 \hat{v}_3 \rangle = 0$ has been assumed (Busse 1970). Then using (C 6) and the fact that $\langle \hat{\boldsymbol{v}} \cdot \delta D/\delta \hat{\boldsymbol{v}} \rangle = 0$ leads to the relationship

$$\frac{Re}{a-1} = \frac{\langle \left(\overline{\hat{v}_1 \hat{v}_3} - h\langle h \hat{v}_1 \hat{v}_3 \rangle\right)^2 \rangle}{8\langle z \hat{v}_1 \hat{v}_3 \rangle}. \tag{C 20}$$

This allows the final variational equation to be solved, (C 10), to be rewritten as

$$\left[\overline{\hat{v}_1 \hat{v}_3} - h\langle h \hat{v}_1 \hat{v}_3 \rangle - \frac{1}{2} \left\{ \sqrt{\mathbb{D}_{lam}} + \frac{\langle \left(\overline{\hat{v}_1 \hat{v}_3} - h\langle h \hat{v}_1 \hat{v}_3 \rangle\right)^2 \rangle}{\langle h \hat{v}_1 \hat{v}_3 \rangle} \right\} h \right] \begin{bmatrix} \hat{v}_3 \\ 0 \\ \hat{v}_1 \end{bmatrix} + \boldsymbol{\nabla} p - \nabla^2 \hat{\boldsymbol{v}} = \boldsymbol{0}, \tag{C 21}$$

which is the Euler–Lagrange equation resulting from Busse's original problem of minimizing

$$\sqrt{\mathbb{D}_{lam}} = \frac{4}{\sqrt{3}} Re = \frac{\langle |\boldsymbol{\nabla} \hat{\boldsymbol{v}}|^2 \rangle}{\langle h \hat{v}_1 \hat{v}_3 \rangle} + \hat{\mu} \frac{\langle \left(\overline{\hat{v}_1 \hat{v}_3} - h\langle h \hat{v}_1 \hat{v}_3 \rangle\right)^2 \rangle}{\langle h \hat{v}_1 \hat{v}_3 \rangle^2} \tag{C 22}$$

at fixed $\hat{\mu} := (\mathbb{D} - \mathbb{D}_{lam})/\sqrt{\mathbb{D}_{lam}}$.

Appendix D

The purpose of this appendix is to show that the Euler–Lagrange problem treated in § 3 (see (3.2)) can be derived directly from the Lagrangian (see (4.3)) used to apply the background method. This means that both variational formulations are striving to estimate the same (highest) stationary point or upper bound. The fact that the Euler–Lagrange problem of § 3 is a maximization problem whereas the Doering–Constantin problem is one of minimization also implies that these formulations represent complementary principles. In this case, a trial function underestimate of the upper bound secured from below using Busse's multiple-boundary-layer technique and a trial background field overestimate of the upper bound allows the correct value to be bracketed.

https://doi.org/10.1017/S0022112002008303 Published online by Cambridge University Press

We illustrate this in the context of PCF by first recalling the Lagrangian of (4.3),

$$\mathscr{L} := f(D - a\langle \boldsymbol{v}\cdot(NS)\rangle, D_m, D_v) = f\left(D - a\langle \boldsymbol{u}\cdot(NS)\rangle + a\int_{-1/2}^{1/2}\phi\overline{(NS)}_1\,\mathrm{d}z, D_m, D_v\right),$$
$$= f(\langle\phi'^2\rangle - \langle(a-1)|\nabla\hat{\boldsymbol{v}}|^2 + (a-1)\bar{v}_1'^2 + a\phi'\hat{v}_1\hat{v}_3 - (a-2)\phi''\bar{v}_1\rangle, \langle(\phi'+\bar{v}_1')^2\rangle, \langle|\nabla\hat{\boldsymbol{v}}|^2\rangle). \tag{D 1}$$

The strategy is to show that if the variational equations

$$\left.\frac{\delta\mathscr{L}}{\delta\phi}\right|_{\bar{v}_1,\hat{\boldsymbol{v}},a} = \left.\frac{\delta\mathscr{L}}{\delta\bar{v}_1}\right|_{\phi,\hat{\boldsymbol{v}},a} = \left.\frac{\delta\mathscr{L}}{\delta a}\right|_{\phi,\bar{v}_1,\hat{\boldsymbol{v}}} = 0 \tag{D 2}$$

are solved then the remaining problem in $\hat{\boldsymbol{v}}$, $\delta\mathscr{L}/\delta\hat{\boldsymbol{v}} = \boldsymbol{0}$, is the Euler–Lagrange equation (3.2). That these three variational equations are implicitly satisfied in that formulation is due to the fact that that the total power and mean momentum balances are built into the Euler–Lagrange problem (3.2) from the beginning,

$$\langle \boldsymbol{u}\cdot(NS)\rangle = 0 \Rightarrow \left.\frac{\delta\mathscr{L}}{\delta a}\right|_{\boldsymbol{u},\phi} = 0, \quad \overline{(NS)}_1 = 0 \Rightarrow \left.\frac{\delta\mathscr{L}}{\delta\phi}\right|_{\boldsymbol{u},a} = \left.\frac{\delta\mathscr{L}}{\delta\phi}\right|_{\bar{v}_1,\hat{\boldsymbol{v}},a} - \left.\frac{\delta\mathscr{L}}{\delta\bar{v}_1}\right|_{\phi,\hat{\boldsymbol{v}},a} = 0, \tag{D 3}$$

and the degeneracy in the velocity representation is implicitly removed by applying

$$\left.\frac{\delta\mathscr{L}}{\delta\bar{v}_1}\right|_{\phi,\hat{\boldsymbol{v}},a} = 0. \tag{D 4}$$

The first of the variational equations in (D 2) leads to the relation

$$[(a-2)f_D - 2f_{D_m}]\bar{v}_1'' + af_D\overline{\hat{v}_1\hat{v}_3}' = 2(f_D + f_{D_m})\phi''. \tag{D 5}$$

Integrating twice and applying the boundary conditions $\bar{v}_1(x, y, \pm\frac{1}{2}) = 0$ means that

$$[(a-2)f_D - 2f_{D_m}]\bar{v}_1' + af_D[\overline{\hat{v}_1\hat{v}_3} - \langle\hat{v}_1\hat{v}_3\rangle] = 2(f_D + f_{D_m})(\phi' + Re). \tag{D 6}$$

Similarly, $\delta\mathscr{L}/\delta\bar{v}_1 = 0$ leads to

$$[2(a-1)f_D - 2f_{D_m}]\bar{v}_1' = [2f_{D_m} - (a-2)f_D](\phi' + Re), \tag{D 7}$$

which allows $\bar{v}_1$ to be eliminated, leaving the relation

$$(\phi' + Re) = \frac{2(a-1)f_D - 2f_{D_m}}{af_D}[\overline{\hat{v}_1\hat{v}_3} - \langle\hat{v}_1\hat{v}_3\rangle]. \tag{D 8}$$

The variational equation $\delta\mathscr{L}/\delta\hat{\boldsymbol{v}} = \boldsymbol{0}$ is

$$af_D\phi'\begin{bmatrix}\hat{v}_3\\0\\\hat{v}_1\end{bmatrix} + \nabla p - 2[(a-1)f_D - f_{D_v}]\nabla^2\hat{\boldsymbol{v}} = \boldsymbol{0}, \tag{D 9}$$

which upon use of (D 8) becomes

$$\left[\frac{(a-1)f_D - f_{D_m}}{(a-1)f_D - f_{D_v}}(\overline{\hat{v}_1\hat{v}_3} - \langle\hat{v}_1\hat{v}_3\rangle) - \frac{Re}{2}\frac{(a-1)f_D + f_D}{(a-1)f_D - f_{D_v}}\right]\begin{bmatrix}\hat{v}_3\\0\\\hat{v}_1\end{bmatrix} + \nabla p - \nabla^2\hat{\boldsymbol{v}} = \boldsymbol{0}. \tag{D 10}$$

This has exactly the form of (3.2) providing $\Lambda = -(a-1)f_D$ (where $(u, v, w) :=$

https://doi.org/10.1017/S0022112002008303 Published online by Cambridge University Press

$(\hat{v}_1, \hat{v}_2, \hat{v}_3)$). This last condition is enforced by imposing the power balance through $\delta\mathscr{L}/\delta a = 0$ and taking $\langle \hat{\boldsymbol{v}} \cdot \delta\mathscr{L}/\delta\hat{\boldsymbol{v}} \rangle = 0$.

REFERENCES

Busse, F. H. 1969*a* On Howard's upper bound for heat transport by turbulent convection. *J. Fluid Mech.* **37**, 457–477.

Busse, F. H. 1969*b* Bounds on the transport of mass and momentum by turbulent flow. *Z. Angew. Math. Phys.* **20**, 1–14.

Busse, F. H. 1970 Bounds for turbulent shear flow. *J. Fluid Mech.* **41**, 219–240.

Busse, F. H. 1972 The bounding theory of turbulence and its physical significance in the case of turbulent Couette flow. In *Statistical Models and Turbulence*. Lecture Notes in Physics, vol. 12, pp. 103–126. Springer.

Busse, F. H. 1978 The optimum theory of turbulence. *Adv. Appl. Mech.* **18**, 77–121.

Busse, F. H. & Joseph, D. D. 1972 Bounds for heat transport in a porous layer. *J. Fluid Mech.* **54**, 521–543.

Caulfield, C. P. & Kerswell, R. R. 2001 Maximal mixing rate in turbulent stably stratified Couette flow. *Phys. Fluids* **13**, 894–900.

Chan, S.-K. 1971 Infinite Prandtl number turbulent convection. *Stud. Appl. Maths* **50**, 13–49.

Chan, S.-K. 1974 Investigation of turbulent convection under a rotational constraint. *J. Fluid Mech.* **64**, 477–506.

Childress, S., Kerswell, R. R. & Gilbert, A. D. 2001 Bounds on dissipation for Navier-Stokes flow with Kolmogorov forcing. *Physica* D **158**, 105–128.

Constantin, P. & Doering, C. R. 1995 Variational bounds on energy-dissipation in incompressible flows: II. Channel flow. *Phys. Rev.* E **51**, 3192–3198.

Constantin, P., Hallstrom, C. & Putkaradze, V. 1999 Heat transport in rotating convection. *Physica* D **125**, 275–284.

Constantin, P., Hallstrom, C. & Putkaradze, V. 2001 Logarithmic bounds for infinite Prandtl number rotating convection. *J. Math. Phys.* **42**, 773–783.

Constantin, P. & Doering, C. R. 1999 Infinite Prandtl number convection. *J. Statist. Phys.* **94**, 159–172.

Doering, C. R. & Constantin, P. 1992 Energy dissipation in shear driven turbulence. *Phys. Rev. Lett.* **69**, 1648–1651.

Doering, C. R. & Constantin, P. 1994 Variational bounds on energy dissipation in incompressible flows: shear flow. *Phys. Rev.* E **49**, 4087–4099.

Doering, C. R. & Constantin, P. 1996 Variational bounds on energy dissipation in incompressible flows: III. Convection. *Phys. Rev.* E **53**, 5957–5981.

Doering, C. R. & Constantin, P. 1998 Bounds for heat transport in a porous layer. *J. Fluid Mech.* **376**, 263–296.

Doering, C. R., Spiegel, E. A. & Worthing R. A. 2000 Energy dissipation in a shear layer with suction. *Phys. Fluids* **8**, 1955–1968.

Doering, C. R. & Constantin, P. 2001 On upper bounds for infinite Prandtl number convection with or without rotation. *J. Math. Phys.* **42**, 784–795.

Doering, C. R. & Foias, C. 2001 Energy dissipation in body-forced turbulence. preprint.

Gebhardt, T., Grossmann, S., Holthaus, M. & Löhden, M. 1995 Rigorous bound on the plane-shear-flow dissipation rate. *Phys. Rev.* E **51**, 360–365.

Gupta, V. P. & Joseph, D. D. 1973 Bounds for heat transport in a porous layer. *J. Fluid Mech.* **57**, 491–514.

Hopf, E. 1941 Ein allgemeiner endlichkeitssatz der hydrodynamik. *Mathematische Annalen* **117**, 764–775.

Howard, L. N. 1963 Heat transport by turbulent convection. *J. Fluid Mech.* **17**, 405–432.

Howard, L. N. 1972 Bounds on flow quantities. *Annu. Rev. Fluid Mech.* **4**, 473–494.

Howard, L. N. 1990 Limits on the transport of heat and momentum by turbulent convection with large scale flow. *Stud. Appl. Maths* **83**, 273–285.

Ierley, G. R. & Malkus, W. V. R. 1988 Stability bounds on turbulent Poiseuille flow. *J. Fluid Mech.* **187**, 435–449.

https://doi.org/10.1017/S0022112002008303 Published online by Cambridge University Press

Ierley, G. R. & Worthing, R. A. 2001*a* Bound to improve: a variational approach to convective heat transport. *J. Fluid Mech.* **441**, 223–253.

Ierley, G. R. & Worthing, R. A. 2001*b* Assessment of a variational theory of turbulence. preprint.

Kerswell, R. R. 1996 Upper bounds on the energy dissipation in turbulent precession. *J. Fluid Mech.* **321**, 335–370.

Kerswell, R. R. 1997 Variational bounds on shear-driven turbulence and turbulent Boussinesq convection. *Physica* D **100**, 355–376.

Kerswell, R. R. 1998 Unification of variational principles for turbulent shear flows: the Background method of Doering-Constantin and Howard-Busse's mean-fluctuation formulation. *Physica* D **121**, 175–192.

Kerswell, R. R. 2000 Lowering dissipation bounds for turbulent shear flows using a smoothness constraint. *Phys. Lett.* A **272**, 230–235.

Kerswell, R. R. 2001 New results in the variational approach to turbulent Boussinesq convection. *Phys. Fluids* **13**, 192–209.

Kerswell, R. R. & Soward, A. M. 1996 Upper bounds for turbulent Couette flow incorporating the poloidal power constraint. *J. Fluid Mech.* **328**, 161–176.

Malkus, W. V. R. 1954 The heat transport and spectrum of thermal turbulence. *Proc. R. Soc.* **225**, 196–212.

Malkus, W. V. R. 1956 Outline of a theory for turbulent shear flow. *J. Fluid Mech.* **1**, 521–539.

Malkus, W. V. R. 1996 Statistical stability criteria for turbulent flow. *Phys. Fluids* **8**, 1582–1587.

Malkus, W. V. R. & Smith, L. M. 1989 Upper bounds on functions of the dissipation rate in turbulent shear flow. *J. Fluid Mech.* **208**, 479–507.

Nickerson, E. C. 1969 Upper bounds on the torque in cylindrical Couette flow. *J. Fluid Mech.* **38**, 807–815.

Nicodemus, R., Grossmann, S. & Holthaus, M. 1997*a* Improved variational principle for bounds on energy dissipation in turbulent shear flow. *Physica* D **101**, 178–190.

Nicodemus, R., Grossmann, S. & Holthaus, M. 1997*b* Variational bound on energy dissipation in plane Couette flow. *Phys. Rev.* E **56**, 6774–6786.

Nicodemus, R., Grossmann, S. & Holthaus, M. 1998*a* The background flow method. Part 1. Constructive approach to bounds on energy dissipation. *J. Fluid Mech.* **363**, 281–300.

Nicodemus, R., Grossmann, S. & Holthaus, M. 1998*b* The background flow method. Part 2. Asymptotic theory of dissipation bounds. *J. Fluid Mech.* **363**, 301–323.

Nicodemus, R., Grossmann, S. & Holthaus, M. 1999 Towards lowering dissipation bounds for turbulent flows. *Eur. Phys. J.* B **10**, 385–396.

Plasting, S. C. & Kerswell, R. R. 2002 Improved upper bound on the energy dissipation in plane Couette flow: The full solution to Busse's problem and the Doering-Constantin problem with 1-D background field. *J. Fluid Mech.* (submitted).

Reynolds, W. C. & Tiederman, W. G. 1967 Stability of turbulent channel flow, with applications to Malkus's theory. *J. Fluid Mech.* **27**, 253–272.

Smith, L. M. 1991 Turbulent Couette flow profiles that maximise the efficiency function. *J. Fluid Mech.* **227**, 509–525.

Vitanov, N. K. 1998 Upper bound on the heat transport in a horizontal fluid layer of infinite Prandtl number. *Phys. Lett.* A **248**, 338–346.

Vitanov, N. K. 2000*a* Upper bounds on the heat transport in a porous layer. *Physica* D **136**, 322–339.

Vitanov, N. K. 2000*b* Upper bounds on the heat transport in a fluid layer of infinite Prandtl number, rigid lower boundary and stress-free upper boundary. *Phys. Rev.* E **61**, 956–959.

Vitanov, N. K. 2000*c* Convective heat transport in a fluid layer of infinite Prandtl number: upper bounds for the case of rigid lower boundary and stress-free upper boundary. *Eur. Phys. J.* B **15**, 349–355.

Vitanov, N. K. 2000*d* Upper bounds on convective heat transport in a rotating fluid layer of infinite Prandtl number: Case of intermediate Taylor numbers. *Phys. Rev.* E **62**, 3581–3591.

Vitanov, N. K. & Busse, F. H. 1997 Bounds on the heat transport in a horizontal fluid layer with stress-free boundaries. *Z. Angew. Math. Phys.* **48**, 310–324.

Vitanov, N. K. & Busse, F. H. 2000 Bounds on the convective heat transport in a rotating layer. *Phys. Rev.* E **63**, 016303(1)–016303(8).

https://doi.org/10.1017/S0022112002008303 Published online by Cambridge University Press

WANG, X. M. 1997 Time averaged energy dissipation rate of boundary driven flows in R^n. *Physica* D **99**, 555–563.

WANG, X. M. 2000 Effect of tangential derivative in the boundary layer on time averaged energy dissipation rate. *Physica* D **144**, 142–153.

WORTHING, R. A. 1990 Assessment of an upper bound theory for turbulent mean flows. MSc Thesis, Michigan Technological University.

https://doi.org/10.1017/S0022112002008303 Published online by Cambridge University Press